
INTERFEROMETRY WITH
BOSE-EINSTEIN CONDENSATES
FROM GROUND TO SPACE

Von der QUEST-Leibniz-Forschungsschule
der Gottfried Wilhelm Leibniz Universität Hannover

zur Erlangung des Grades

Doktor der Naturwissenschaften
– **Dr. rer. nat.** –

genehmigte Dissertation von

M. Sc. Dennis Vincent Daniel Becker

2021

Referent: **Prof. Dr. Ernst M. Rasel**
Institut für Quantenoptik
Leibniz Universität Hannover

Korreferent: **Prof. Dr. Wolfgang Ertmer**
Institut für Quantenoptik
Leibniz Universität Hannover

Korreferent: **Prof. Dr. Kai Bongs**
School of Physics and Astronomy
University of Birmingham

Tag der Promotion: **05.10.2021**

Abstract

Quantum sensors based on atom interferometry are precise measurement devices whose ultimate performance can be reached using Bose–Einstein condensates (BECs) in extended free fall. This thesis summarizes the endeavour of the QUANTUS and MAIUS collaborations to enable BECs for precision interferometry in space. To this end, an atom-chip setup was developed to efficiently produce BECs of Rb-87 atoms in a compact and robust apparatus. Two different microgravity facilities, the ZARM drop tower and a sounding rocket, were utilized to serve as test-beds for future orbital space missions. The first generation drop tower experiment QUANTUS-1 performed BEC-based atom interferometry in microgravity realizing interferometer times of up to 677 ms. The successor QUANTUS-2 setup was improved to realize a high-flux source producing BECs of 4×10^5 atoms in 1.6 s. The advanced setup provides excellent control over the BECs and reaches a pointing reproducibility on the low μm level as required by future space-based atom interferometry missions. In combination with simulations based on a detailed atom-chip model this allowed employing sophisticated protocols for the transport of the atoms on the chip and reducing the expansion energy of the BEC to 38 pK thus enabling extended free-fall times of up to 2.7 s. The atom-chip setup was next used as the basis for the design of the scientific payload MAIUS-A to be operated on a sounding rocket flight. A comprehensive qualification and verification throughout the process ensured that the apparatus would fulfil the requirements set by the rough environment of a sounding rocket mission. The robustness of the system and the high BEC flux of 10^5 atoms/s allowed conducting 110 experiments central to matter-wave interferometry in the course of the rocket flight MAIUS-1. The implemented sequence graph based on onboard evaluation enabled the autonomous operation of the measurements as well as the optimization of key parameters during the space flight. In particular, the phase transition into the BEC was analysed and the BECs were studied as a source for high-precision atom interferometry. Indeed, the dynamics of the collective evolution of the BEC during transport and free expansion for up to 300 ms were analysed. The measurements showed an instability of 1 % and results in agreement with mean-field simulations. These simulations are based on the atom-chip model and take gauged uncertainties of the applied currents and the geometric dimensions of the setup into account. Furthermore, a variety of experiments on Bragg diffraction and shear interferometry investigating the coherence of the BEC were conducted. The development of the hardware technology and the successful demonstration of all of these atom-optic methods represents an important milestone for high-precision atom interferometry with BECs in space. The presented results have set the foundation for future space missions aiming at geodesy applications or tests of fundamental physics.

Key words: atom interferometry, Bose-Einstein condensation, microgravity, space

Contents

1 Introduction	1
1.1 Publications	3
2 Atom interferometry	5
2.1 Extended free fall	7
2.2 Bose-Einstein condensation	8
3 Bose-Einstein condensates for microgravity	11
3.1 QUANTUS-1: Atom interferometry in the drop tower	12
3.2 QUANTUS-2: High-flux BEC source for atom interferometry	15
4 Atom interferometry in space	21
4.1 MAIUS-A: Design and qualification of scientific payload	22
4.2 MAIUS-1: Sounding rocket flight campaign	25
5 Conclusion	33
Bibliography	37

CHAPTER 1

Introduction

Interferometry is an exquisite measurement technique based on the superposition principle of waves. Since decades, interferometry has a high impact in the fields of astronomy, biology, chemistry, engineering, and physics. Today, optical interferometers are widely used both in science and in industry for precision measurements, e.g. for the detection of gravitational waves [1, 2] or to measure the rotation of the Earth [3].

By utilizing the wave character of particles [4], it is also possible to use cold atoms [5, 6] as an input state for interferometry [7]. Similar to their optical counterparts, atom interferometers measure the accumulated phase difference between matter waves along different paths [8]. Atom interferometers have been used to test fundamental physics including measurements of the gravitational constant [9, 10], the fine-structure constant [11, 12], and the universality of free fall [13–18]. The latter allows searching for a "theory of everything" [19] by probing general relativity [20] with quantum objects [21]. Recently, atom interferometers also have been proposed as a method to detect gravitational waves [22–26]. Furthermore, atom interferometry found application in inertial sensing of accelerations [27] or rotations [28–30] and Earth observation via gravimetry [31–36] or gravity gradiometry [37, 38].

The urge to further improve our understanding of the Universe makes it essential to keep increasing the precision of the measurements. The sensitivity of an interferometer typically scales quadratically with the free-fall time of the atoms and thus can be drastically enhanced by extended free fall as experienced in fountain [39, 40] or microgravity [41, 42] experiments. In particular, a spacecraft provides not only microgravity but also a quiet and seismic-noise free environment and thus presents an excellent platform for high-precision measurements [23, 43–45]. To fully exploit the long interferometry times possible it is indispensable to have an ultra-cold atomic ensemble with a vanishingly low expansion velocity. Although this requirement can be fulfilled with Bose-Einstein condensates (BECs) [46–51] in combination with further delta-kick collimation (DKC) [41, 52, 53], it is technically challenging and demands high effort.

In early 2004 the QUANTUS (Quantum Gases in Weightlessness) collaboration, comprised of several universities and funded by the German Aerospace Center DLR, was initiated with the goal to bring BECs into space and thus enabling high-precision

matter-wave interferometry for research in both fundamental physics and Earth observations [54]. The biggest challenge was to get the typically lab-filling setups for the creation of BECs to be compact and robust enough to be deployed in microgravity facilities, e.g. drop towers or sounding rockets. By employing special diode lasers [55, 56] and atom chips consisting of micro integrated current structures [57–59] for cooling and trapping of the atoms, it was possible to create BECs for the first time in microgravity [60] and subsequently in space [61]. The comparable easier access of drop towers and sounding rockets made these experiments an ideal test-bed for new technologies and atom-optical methods [62–64] required for the success of future satellite missions [43, 65] performing atom interferometry to extend our knowledge on fundamental physics and of the Earth.

Scope of this thesis

This thesis presents the endeavour of the QUANTUS collaboration to enable BECs for precision interferometry in space. At first, a short introduction to atom interferometry (chap. 2) is given. Herein, the advantageous of performing the atom interferometer in extended free fall with BECs as a source are highlighted. Based on that, the pioneering work of the drop tower experiments QUANTUS-1 and -2 for BEC-based atom interferometry in microgravity is presented (chap. 3). In particular, the conducted atom interferometry over extended free-fall times in the drop tower (Ref. [A1]) and the developed high-flux BEC source (Ref. [A2]) are discussed. The next chapter describes the design and qualification of the scientific payload MAIUS-A (chap. 4), with a focus on the vacuum system (Ref. [A3]) in which the experiments are performed. Chapter 4 furthermore presents the experimental results of the sounding rocket mission MAIUS-1 (Ref. [A4, A5]), highlighting the study of the space-borne BEC for precision interferometry. The thesis concludes (chap. 5) with a discussion of the results achieved within this work and its impact on current and future space-borne atom interferometry missions.

1.1 Publications

This thesis is based on the following original publications:

- A1. H. Müntinga, H. Ahlers, M. Krutzik, A. Wenzlawski, S. Arnold, **D. Becker**, K. Bongs, H. Dittus, H. Duncker, N. Gaaloul, et al.: ‘Interferometry with Bose-Einstein condensates in microgravity’. *Physical review letters* (2013), vol. 110(9): p. 093602 (cit. on pp. 2, 12, 13).

Contribution: As a member of the QUANTUS collaboration, I supported the experimental team, consisting of H. M., H. A., M. K., and A. W., in the data evaluation.

- A2. J. Rudolph, W. Herr, C. Grzeschik, T. Sternke, A. Grote, M. Popp, **D. Becker**, H. Müntinga, H. Ahlers, A. Peters, et al.: ‘A high-flux BEC source for mobile atom interferometers’. *New Journal of Physics* (2015), vol. 17(6): p. 065001 (cit. on pp. 2, 15, 16, 18, 30).

Contribution: I helped J. R. and W. H. setting-up the experiment, optimizing the loading scheme and performing the measurements.

- A3. J. Grosse, S. T. Seidel, **D. Becker**, M. D. Lachmann, M. Scharringhausen, C. Braxmaier, and E. M. Rasel: ‘Design and qualification of an UHV system for operation on sounding rockets’. *Journal of Vacuum Science & Technology A: Vacuum, Surfaces, and Films* (2016), vol. 34(3): p. 031606 (cit. on pp. 2, 24).

Contribution: Alongside J. G. and S. T. S. I set up the vacuum system and performed the vibrational tests.

- A4. **D. Becker**, M. D. Lachmann, S. T. Seidel, H. Ahlers, A. N. Dinkelaker, J. Grosse, O. Hellmig, H. Müntinga, V. Schkolnik, T. Wendrich, et al.: ‘Spaceborne Bose-Einstein condensation for precision interferometry’. *Nature* (7727 2018), vol. 562: pp. 391–395 (cit. on pp. 2, 23, 25–28).

Contribution: Together with M. D. L., S. T. S., and others I planned and executed the campaign, carried out the data evaluation and the simulations, and wrote the manuscript.

- A5. M. D. Lachmann, H. Ahlers, **D. Becker**, A. N. Dinkelaker, J. Grosse, O. Hellmig, H. Müntinga, V. Schkolnik, S. T. Seidel, T. Wendrich, et al.: ‘Ultracold atom interferometry in space’. *Nature Communications* (2021), vol. 12: p. 1317 (cit. on pp. 2, 29, 30).

Contribution: Together with M. D. L., S. T. S., and others I planned and executed the campaign. I supported M. D. L. and H. A. evaluating the data.

CHAPTER 2

Atom interferometry

All sensors mentioned in this thesis are based on the principle of light-pulse atom interferometry. These atom interferometers are comprised of beam splitters and mirrors analogue to classical light interferometers. Here, counter-propagating laser beams are creating a grating made of light which is diffracting the atoms. This interaction with light coherently transfers the atoms by a two-photon process from state $|1\rangle$ via a detuned intermediate state to state $|2\rangle$. The hereby transferred momentum $\vec{p} = \hbar\vec{k}_{\text{eff}}$ is proportional to the effective two-photon laser wave vector \vec{k}_{eff} and the reduced Planck constant \hbar . Depending on the configuration of this process, the atoms either stay in the same electronic state (Bragg) [66, 67] or are transferred to a different internal state (Raman) [68, 69]. By properly adjusting the pulse strength, given by the product of the pulse duration t and the Rabi frequency (Ω), the transferred population can be set to $1/2$ ($\Omega t = \pi/2$) or 1 ($\Omega t = \pi$). The beam splitter and mirror pulses are thus called $\pi/2$ and π pulse, respectively.

With a sequence of $\pi/2$ and π pulses separated by a time T different types of interferometers can be formed: The Ramsey interferometer, comprised of two $\pi/2$ pulses, is widely used to determine the transition frequency in atomic clocks and can also be applied to measure the velocity of the atomic cloud. The $\pi/2 - \pi - \pi/2$ sequence resulting in a Mach-Zehnder type geometry (see fig. 2.1) can be used to precisely measure rotation $\vec{\Omega}$ [70] or acceleration \vec{a} [71]. Additional pulses can be added to the common interferometer sequences to suppress disturbing effects or to enhance the sensitivity on the measurement quantity, e.g. Ramsey-Bordé interferometer or Mach-Zehnder interferometer in a $\pi/2 - \pi - \pi - \pi/2$ butterfly configuration. Multiple interferometers can also be employed in a differential setup, e.g. as a gravity gradiometer, to measure alternating forces, or to test the weak equivalence principle with either different atomic species, isotopes of the same species, or internal states of the same atomic source.

In all these cases, a phase difference between the two paths accumulates due to internal and external effects during the interferometer sequence. For a Mach-Zehnder interferometer this leads to a phase difference of

$$\Delta\phi = (\vec{k}_{\text{eff}} \cdot \vec{a} + 2(\vec{k}_{\text{eff}} \times \vec{v}) \cdot \vec{\Omega})T^2 \quad (2.1)$$

with \vec{v} as the velocity of the atoms.

At the end of the sequence the phase difference can be determined by measuring the ratio of the populations N_0 and N_1 in the output ports. The measurement of the atom number N is limited due to the quantum projection noise. This leads to a lower bound for the phase uncertainty $\Delta\phi \propto 1/\sqrt{N}$. Hence, a large number of atoms is favourable for an interferometer to reach a good single shot sensitivity. All variables in the measurement, pulse separation time T and effective laser wave vector \vec{k}_{eff} , can be related to a well-known frequency standard and the quantity of interest can therefore be precisely measured with a light-pulse atom interferometer.

However, systematic errors are limiting the interferometric measurement and can lead to incorrect results. These include e.g. gravity gradients, residual non-linear magnetic fields, or distortions in the wavefront of the interferometry beams. Most of the errors scale with the center of mass motion and expansion velocity of the atomic cloud. A high level of control on the motion of the atoms and a low expansion velocity are therefore essential ingredients for a high-precision measurement. Random fluctuations of external effects or in the prepared atomic source can be averaged down by repeated measurements. Employing a high-flux source in the interferometer enables a high repetition rate and reduces the statistical uncertainties of the measurement.

Performing a Mach-Zehnder type interferometer with a small difference δT between the two pulse separation times will result in a spatial displacement d in each output port. Such an asymmetric Mach-Zehnder interferometer (AMZI) has, similar to the Ramsey interferometer [72], spatial fringes on the two output ports and is comparable to a double-slit experiment [73]. With the AMZI it is possible to study the temporal coherence of the atomic cloud and to evaluate the contrast of a Mach-Zehnder type interferometer in a single measurement. The fringe spacing will linear increase with the total expansion time of the atomic clouds and is inversely proportional to the displacement d .

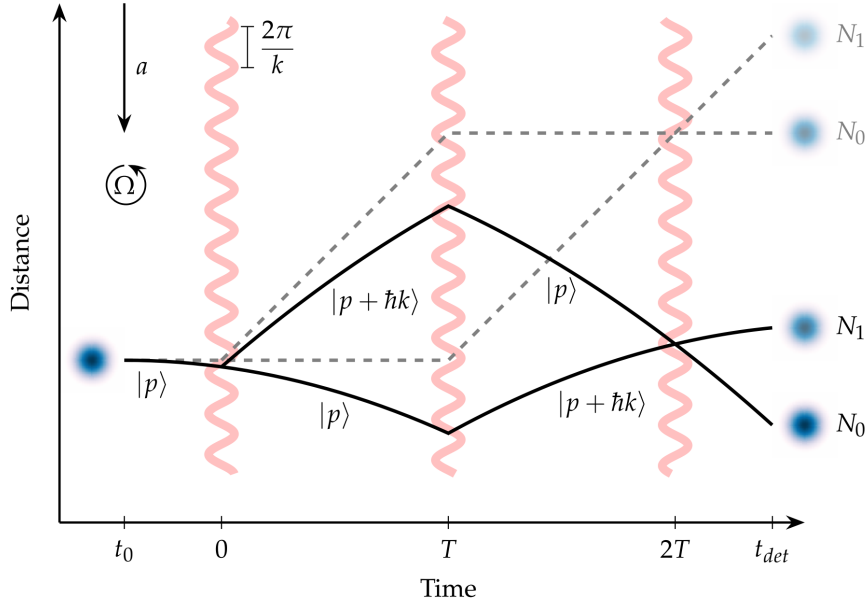


Figure 2.1: Mach-Zehnder type interferometer. A cloud of atoms (blue circle) is prepared and released at t_0 . The light beams (red sinusoidal lines) coherently split and recombine the atom trajectories depicted for an acceleration $a > 0$ (solid) and for microgravity $a = 0$ (dashed). The acceleration a or rotation Ω acting on the atoms can be determined by the detected population difference of the two output states N_0 and N_1 . Taken from [74].

2.1 Extended free fall

As seen from (2.1) the sensitivity scales quadratically with the pulse separation time T . To increase the pulse separation and gain sensitivity it is necessary to extend the free-fall time of the atoms. There are two concepts on how to extend the free-fall time in an atom interferometer: On the one hand there are fountain experiments, e.g. atomic fountain clocks, where atoms are accelerated upwards and then travel along the trajectory following the gravitational field. On the other hand there are microgravity experiments where the entire experiment carries out a parabolic flight and the atoms are set at rest in respect with the experiment.

Both methods certainly have their own advantages and drawbacks. The optimal setup also strongly depends on the environment and the value to be measured. Smaller fountain experiments (length $l < 1\text{ m} \Rightarrow T < 0.5\text{ s}$) are practical in a mobile setup for field applications [34]. Stationary and larger fountain setups ($l = 1\text{ m} - 10\text{ m} \Rightarrow T = 0.5\text{ s} - 3\text{ s}$) deliver higher sensitivities and are best for gravitational reference measurements or tests of fundamental physics [39, 40, 75]. Microgravity experiments on orbital platforms can be utilized both for geodetic Earth observations or for tests of fundamental physics at ultra-long time scales ($T > 1\text{ s}$).

Table 2.1: Comparison of microgravity facilities. The Bremen Drop Tower operated by ZARM [76] provides 10 launches per week. The Einstein-Elevator [77] at the Hannover Institute of Technology supports 300 launches per day. The Novespace Zero-G airplane [78] is available for 5-7 campaigns per year each consisting of 2-4 flights with 30 parabolas per flight. The Esrange Space Center [79] conducts about 10 sounding rocket missions per year each providing 6 minutes of μg . On the International Space Station (ISS) an experiment typically operates 40 h per week. On a dedicated satellite an experiment can run continuously. For orbital facilities the duration of the μg phase is only limited by the experiment itself.

microgravity facilities	quality $\delta a/g_0$	duration sec	availability h/year
Zarm drop tower	10^{-6}	9	1.3
Einstein-Elevator	10^{-5}	4	87
Zero-G airplane	10^{-2}	22	3.3
sounding rocket	10^{-6}	360	1
ISS	10^{-4}	—	2000
satellite	10^{-6}	—	8760

They are also especially suited for differential measurements because the atomic clouds stay stationary inside the experiment before and during the interferometer.

Although orbital platforms offer the best conditions for ultra-high precision measurements they also come with very high financial demands and a variety of challenges. Other available microgravity platforms like Earth-bound drop towers or sounding rockets deliver similar high-quality microgravity conditions with much better accessibility (see table 2.1). This is why these platforms qualify as a perfect test bed for highly anticipated dedicated satellite missions.

2.2 Bose-Einstein condensation

In order to profit from the long free-evolution times provided by the microgravity facilities it is indispensable to have an atomic source with very low expansion velocities. In most of the smaller fountain experiments thermal clouds of a few microkelvins are used as an input state. These temperatures are realized with polarization gradient cooling [80] and result in expansion velocities $\sigma_v \approx 50$ mm/s. With additional velocity selection based on light pulses blowing away all but the slowest atoms it is still possible to work with these thermal atoms for up to a few hundred milliseconds at the cost of a reduced atom number. The velocity selection technique certainly works comfortably for small fountain experiments but will be unfavourable at longer interferometry times. These require lower expansion velocities and would result in even lower atom numbers.

As an alternative and more direct approach, very low expansion velocities can

be achieved by active cooling of the atoms. In the case of Bosons this will result below a density dependent critical temperature in a special macroscopic state of matter, the Bose-Einstein condensate [46–51]. Besides their fascinating properties, e.g. superfluidity and quantum vortices [81], BECs also offer many advantages for precision atom interferometry: The initial size of the cloud is much smaller because all the atoms are occupying the ground state in a potential. Furthermore, the atomic cloud has typically a much slower expansion rate and a large coherence length that extends over the entire cloud. Furthermore, utilizing BECs as a source for atom interferometry reduces systematic uncertainties such as inhomogeneous dephasing due to field gradients and wavefront distortions [82].

To further cool the atoms from the few microkelvins after polarization gradient cooling to the critical temperature, usually at around 100 nK, evaporative cooling is applied. This process continuously removes only the most energetic atoms and lets the cloud rethermalize until it reaches the critical temperature. To compete with the standard velocity selection technique this process needs to be both fast and efficient. In the past decade several new methods for state preparation and cooling have been developed. Advancements in technology, e.g. atom chips or acousto-optic deflectors, help to create optimized trapping potentials. In combination these enable setups for fast and efficient evaporation resulting in a high BEC flux. The high level of control and the high flux that can be achieved with BEC experiments make them promising candidates for high-precision atom interferometry.

CHAPTER 3

Bose-Einstein condensates for microgravity

The QUANTUS collaboration follows the goal to bring BECs into space and thus enabling high-precision research in both fundamental physics and Earth observations. The biggest challenge was to get the typically lab-filling setups to create BECs to be sufficiently robust and compact to be deployed in a drop tower or other microgravity facilities. The here utilized Bremen Drop Tower operated by the Center of Applied Space Technology and Microgravity (ZARM) has a 110 m long drop tube and provides 4.7 s in drop or 9.3 s of microgravity in catapult mode [76]. Operating an experiment in the drop tower sets stringent restrictions on volume and mass, which could not be fulfilled with any lab-based BEC experiment. Furthermore, strong loads and forces act on the setup during launch and impact.

With the QUANTUS-1 apparatus the first fully-functional BEC experiment for the drop tower has been build. The experimental setup is based on a typical magneto-optical trap (MOT), which is loaded from a rubidium (Rb) background vapour, combined with a sophisticated atom-chip setup for BEC production. The atom chip consists of several integrated micro structures and is situated inside the vacuum chamber. With the atom chip it is possible to magnetically trap the atoms and perform radio frequency based forced evaporation. Because it is close to the atoms the required magnetic potentials can be generated with comparable low currents at low voltages which reduces the overall power consumption of the setup. Crucial parameters of the evaporation process, e.g. trapping frequency, trap bottom, or cut-off frequency, can be independently adjusted for an efficient evaporation. The apparatus furthermore has a compact and robust laser system to be able to operate in the drop tower.

The QUANTUS-1 apparatus accomplished the first demonstration of a BEC in microgravity in 2007 [60]. Following, QUANTUS-1 conducted further drop campaigns to study the BEC evolution and to perform BEC-based atom interferometry in microgravity (section 3.1). Based on the successful results of QUANTUS-1, a second generation experiment with enhanced capabilities was build. The QUANTUS-2 apparatus was set up as a smaller capsule to support the catapult mode of the drop tower and to extend the microgravity time to the full 9.3 s. The setup included an advanced three-layer atom chip for fast and efficient evaporation (section 3.2).

Moreover, it was designed as a two-species experiment to perform tests of the weak equivalence principle [83].

This chapter describes first the results and challenges performing atom interferometry with QUANTUS-1 in the drop tower and following this the design and setup of the second generation experiment QUANTUS-2 as a high-flux BEC source for atom interferometry. Further details and in-depth descriptions about the hardware and the experimental results of both QUANTUS-1 and -2 can be found in the corresponding dissertations of my colleagues [74, 84–92].

3.1 QUANTUS-1: Atom interferometry in the drop tower

After reliable production of BECs in the drop tower was established, the drop campaigns were targeted at studying the free expansion of the BEC [60]. To be able to detect the atoms after a time of flight in the order of one second it is necessary to reduce the expansion velocity of the BEC. For this the technique of delta-kick collimation (DKC) [93] is employed. After a short free expansion of the atomic cloud a trapping potential is applied for a brief moment. By this, the kinetic energy of the atomic cloud can be drastically reduced. To mitigate disturbing external magnetic forces on the atomic cloud during its expansion after DKC a state preparation has been implemented. The adiabatic rapid passage (ARP) [94] transfers the atoms into the magnetically insensitive state $|m_F\rangle = 0$. With these experimental techniques the BEC can still be detected after free expansion times of up to two seconds, limited by the microgravity time in the drop tower itself.

Following the optimization of the release and the DKC, the next goal was to perform BEC-based atom interferometry in microgravity. As a first step studies on spatial coherence based on a two-pulse Ramsey interferometer were conducted. A spatial fringe structure on the atomic cloud appears after the interferometry sequence. From a single experimental run one can determine the fringe spacing and the contrast of the measurement. When performing a Mach-Zehnder type interferometer only the population difference of the two output ports can be measured. To determine the contrast and the phase offset of the measurement a phase scan is required. Here, the phase of the interferometer is varied over a full oscillation cycle. This can be overcome by introducing a small difference δT to one of the pulse separation times and thus creating an asymmetric Mach-Zehnder interferometer (AMZI) [A1] with spatial fringes on the two output ports. With this scheme it is possible to evaluate the contrast of a Mach-Zehnder type interferometer in a single measurement. For QUANTUS-1 the AMZI scheme is highly beneficial since the drop tower only allows for up to three drops per day.

The AMZI paired with the technique of DKC allowed probing the coherent evolution of the BEC in extended free fall (see fig. 3.1). The high coherence of the BEC itself resulted in a high contrast even for expansion times for up to one second. For an

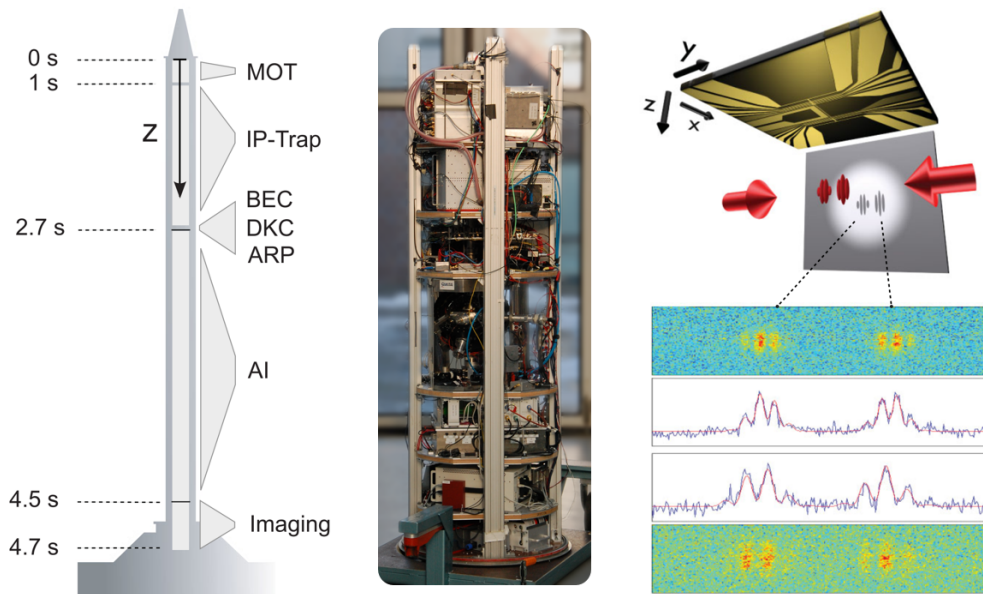


Figure 3.1: Atom interferometry in the drop tower. Left: experimental sequence as performed during the 4.7 s of μg in the Bremen Drop Tower. Center: photo of the QUANTUS-1 capsule. Top right: illustration of the atom chip with atomic clouds in the two output ports of the AMZI realized by two counter-propagating light beams depicted as red arrows. Bottom right: resulting interference patterns are visible in the taken absorption pictures and in the corresponding line integrals of the density distribution. Adapted from [A1].

interferometry time of up to 500 ms the contrast was constant at around 50 %. For longer times the contrast started to decrease. After a total interferometer time of 677 ms a fringe structure was still visible with a contrast of 20 %. The applied pulse separation times of up to 330 ms correspond to a macroscopic spatial separation of the wave packets during the interferometer of up to 2 mm.

To identify the reason for the loss of contrast an extensive study was performed. For this a variety of additional measurements were conducted both with the AMZI and a Ramsey interferometer for comparison. First, a new type of detection scheme was implemented to exclude a low signal to noise ratio as the source of the contrast decrease. To test the influence of wave front errors measurements with varying beam configurations were performed. After ruling out these two setup-specific sources as a next step external disturbances were investigated. The effect of magnetic fields on the atoms was tested by utilizing mixtures of different $|m_F\rangle$ states as an input for the interferometer. Another possible reason for a loss of contrast are rotations introduced on the apparatus due to the release mechanism of the drop tower. An inertial measurement unit was installed in the capsule to track rotations during the drop. The measured rotations explained the observed tilt of the interferometry fringes

but were more than one order of magnitude too low to result in the experienced loss of contrast. Even after all the conducted measurement no conclusive result was obtained to explain the decrease in contrast.

Discussion of results

The achieved results of the AMZI scheme utilized to study the coherence of the BEC in extended free fall were quite remarkable during that time and opened up a rather unexplored field. The AMZI has since been used in a variety of experiments to probe different effects. It has been implemented to measure rotations and accelerations as a three-axes inertial sensor [95] as well as to probe the space-time curvature over the extent of the atomic ensemble [96]. Many other groups are working on interferometry in extended free fall, e.g the microgravity experiment ICE from France and the long-baseline fountain experiment situated in Stanford, USA.

The ICE experiment is designed as a two-species interferometer working with cold atoms of Rb and K. The low temperatures are reached by polarization gradient cooling only. The measurements are performed during several consecutive parabolic flights inside the Novespace Zero-G airplane [78]. Each parabola provides 22 seconds of microgravity but the achievable interferometry time is limited to several milliseconds due to the comparable large residual accelerations of 1×10^{-2} g. This setup realized a dual-species interferometer with pulse separation times of 2 ms with a contrast of 4% [97]. To improve the measurements they have set up a second generation experiment including an optical dipole trap for evaporative cooling. The new setup is currently being tested in a miniature active drop tower allowing for around one second of microgravity time [98].

The apparatus in Stanford is based on a 10 m long baseline which in a fountain geometry results in a free-fall time of around 2.5 s. The experiment works with the two isotopes Rb-85 and Rb-87 and has performed interferometry with either cold thermal clouds or BECs. Additional steps of state preparation and DKC have been implemented to reach low expansion velocities and long time of flights. They have shown long interferometry times of up to 2.3 s for inertial measurements [95, 99] and 2.1 s for a test of macroscopic quantum superposition [75]. The setup has also been used in a differential configuration as a gravity gradiometer [100] and for a test of the weak equivalence principle at the 10^{-12} level [40].

Although the achieved interferometry time of the fountain experiment has surpassed the numbers of QUANTUS-1 it is important to keep the results in perspective: The Stanford experiment is working since several years and unlike to the drop tower a continuous operation with thousands of measurements per day is possible. However, as the fountain experiment is based on a different technology approach it can not be easily adapted for a space mission. After achieving the interferometry results QUANTUS-1 stopped with the drop tower experiments because both the maximum in performance of the setup and in interferometry time possible in the drop mode

had been reached. The experiment is since working as a ground-based test-bed developing new techniques, e.g. large momentum transfer [101, 102] or differential atom interferometry [103], crucial for future atom interferometry space missions.

3.2 QUANTUS-2: High-flux BEC source for atom interferometry

Based on the successful demonstration of the first BEC in microgravity with the QUANTUS-1 experiment a second generation drop tower experiment was planned and built. The QUANTUS-2 setup (see fig. 3.2) is even more compact and robust and fits into a smaller drop tower capsule. With this configuration it can be operated in the catapult mode of the drop tower enabling up to 9.3 s of microgravity time. The experimental setup of QUANTUS-2 is based on its predecessor with a variety of upgrades and additional capabilities: It is designed as a dual-species atom interferometer utilizing ultra-cold Rb and K atoms. The light for cooling and manipulation of the atoms is provided by a new generation laser system build on micro-integrated laser modules [104]. Power supply and control of the experiment are realized by mainly digital and self-built electronics. The vacuum section is based on a two-chamber setup optimized for a higher flux. This enables loading the MOT during the free flight as necessary for the catapult mode. The setup also has an improved multi-layer atom chip integrated for fast and efficient evaporation. The new chip furthermore allows for enhanced control of the atoms enabling advanced state preparation and DKC protocols. Additionally, the vacuum chamber is surrounded by a double-layer magnetic shield to minimize external disturbances.

With all these implemented advancements it was possible to produce a large BEC of 4×10^5 atoms in just 1.6 seconds [A2], improving on the QUANTUS-1 experiment in both realized atom number and required preparation time by one order of magnitude. The experimental sequence to produce a BEC in QUANTUS-2 consists of five steps: (1) First a beam of cold atoms is generated in the 2D-MOT chamber. The atoms are directed through a differential pumping stage into the science chamber to load the 3D-MOT directly on the atom chip. The 3D-chip-MOT is set up in a mirror-MOT configuration using only four cooling beams and the reflective surface of the chip as a mirror. Typically a MOT with 1×10^9 atoms is loaded in a few hundred milliseconds. (2) Afterwards, several preparation techniques are applied to efficiently transfer the atoms into a magnetic trap. These include compressing the MOT and moving it closer to the atom chip, polarization gradient cooling to reduce the ensemble temperature to a few μK , and optical pumping to the magnetic susceptible $|m_F = 2\rangle$ state. (3) After the state preparation 2×10^8 atoms are loaded into the initial Ioffe-Pritchard type trap (IP-trap) generated by a combination of mesoscopic and microscopic wire structures on the atom chip. (4) Next, the atoms are smoothly transferred into another magnetic trap configuration produced by solely microscopic structures. This trap is much closer to the atom chip and trap frequencies of several kHz can be

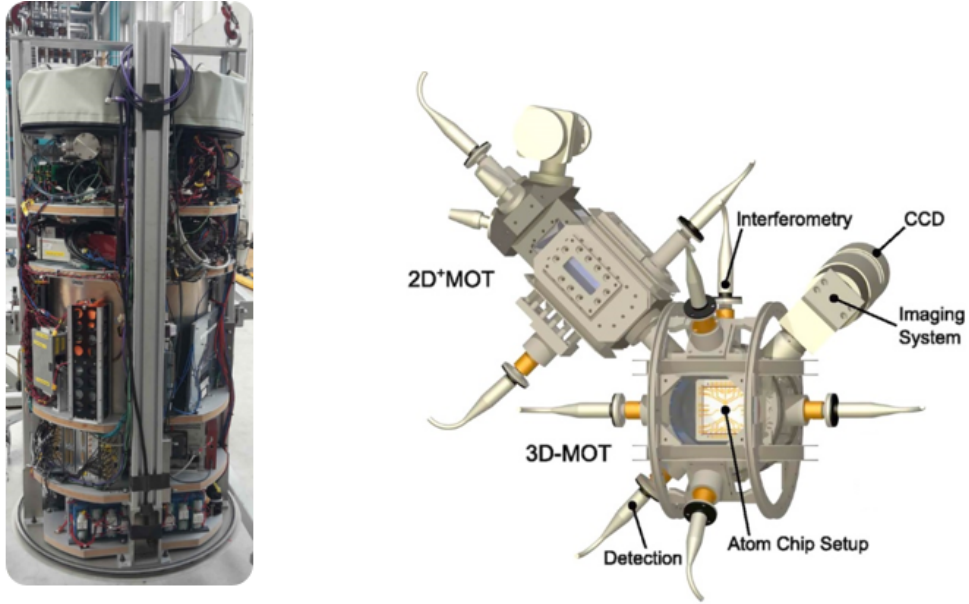


Figure 3.2: High-flux BEC source. Left: photo of the QUANTUS-2 capsule. Right: CAD model of the vacuum system with the atom chip inside. The 2D-MOT generates a cold atomic beam to load the 3D-MOT. The atom-chip setup is utilized to trap and further cool the atoms to degeneracy. With this high-flux setup BECs of 4×10^5 atoms can be produced in 1.6 s. Adapted from [A2].

realized. The tight trap provides high elastic collision rates of around 500 Hz and thus an excellent starting point for efficient evaporative cooling. (5) The forced evaporation is based on several consecutive radio-frequency ramps. A microscopic structure on the atom chip is used for the radiation and parameters like the duration, frequency step and amplitude are optimized for each ramp. The trapping potential can also be altered to adapt the collision rates for an optimal result. The achieved evaporation efficiency of $\gamma = 3.34$ is close to the calculated maximum and highlights the performance of the system.

Due to the versatility of the atom chip the cycle time can be adjusted for a given application: For an experiment interested in a very short preparation time a BEC of 4×10^4 atoms can be generated in just 850 ms. With a repetition rate of 1 Hz BECs with 1×10^5 atoms can be produced, which is useful for e.g. mobile atom interferometers. For QUANTUS-2 the high repetition rate especially helps for the study of the BEC, as multiple measurements can be taken during one drop. In a single catapult launch four BECs were produced in a row and their free expansion was analyzed (fig. 3.3). Due to issues with loose particles floating inside the vacuum chamber when using the catapult launch, further studies have been carried out in

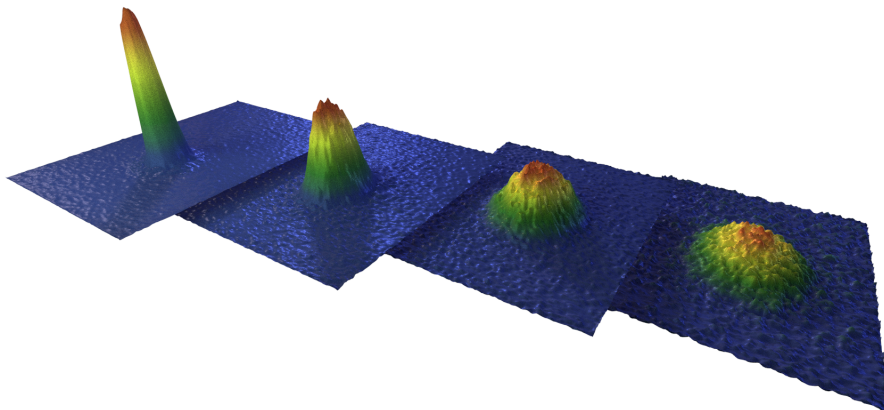


Figure 3.3: Time of flight series of a BEC. During one catapult launch four BECs were produced with the QUANTUS-2 setup. Shown are the corresponding absorption pictures of the four BECs taken after free time of flights of 25 ms, 50 ms, 75 ms and 100 ms (left to right).

the drop mode. First, the procedure to transport the BEC away from the atom chip has been optimized to reduce residuals oscillations. For this, advanced protocols, e.g. shortcut to adiabaticity [63, 105] and optimal control theory [106, 107], have been utilized. In the next drop campaigns, the release and the DKC was analysed and by the means of theoretical models optimized. With a combination of well timed quadrupole oscillation modes of the BEC and additional DKC it was possible to reach expansion velocities corresponding to tens of pK in all three dimensions [108]. The high BEC flux and the ultra-low expansion temperature enable QUANTUS-2 to utilize the full potential of the drop tower. So far QUANTUS-2 has already shown time of flights of up to 2.7 seconds with a high signal to noise ratio using the drop mode which could be extended to free evolution times of up to 8 seconds in the catapult mode.

Discussion of results

The high BEC flux achieved with the compact and mobile QUANTUS-2 setup marked an important milestone for atom interferometry both in space and field applications. A high flux is one key ingredient for the success of space missions performing atom interferometry or other experiments with ultra-cold atoms. In a sounding rocket flight only a limited time of microgravity is available. The number of measurements is therefore directly dependent on the production time of the BEC. For an experiment

Table 3.1: Comparison of BEC production times. From the number of atoms in the BEC (N) and the total production time of the BEC (t) a BEC-flux (Φ) can be calculated for the different setups based on atom chips, dipole traps, or hybrid traps, working with alkali or earth-alkaline atoms, and for mobile or lab operation.

experiment	N 10^5	t s	Φ $10^5/\text{s}$	species	setup	operation
QUANTUS-2 [A2]	4	1.6	2.5	^{87}Rb	chip	mobile
QUANTUS-2 [A2]	1	1	1	^{87}Rb	chip	mobile
Farkas et al. [109]	0.15	1	0.15	^{87}Rb	chip	mobile
Condon et al. [98]	0.4	13.5	0.03	^{87}Rb	dipole	mobile
Clement et al. [110]	1.5	7	0.21	^{87}Rb	dipole	lab
Kinoshita et al. [111]	3.5	3.3	1.06	^{87}Rb	dipole	lab
Yamashita et al. [112]	12	6.1	1.97	^{87}Rb	dipole	lab
Colzi et al. [113]	70	30	2.33	^{23}Na	hybrid	lab
Roy et al. [114]	1	1.8	0.56	^{174}Yb	dipole	lab
Stellmer et al. [115]	1	2	0.5	^{84}Sr	dipole	lab
Stellmer et al. [115]	110	50	2.2	^{84}Sr	dipole	lab

on an orbital platform, e.g. satellite or space station, not the microgravity time but the mission duration is the limiting factor. A shorter production time allows for faster averaging and to tackle leading systematics of the measurement. The high BEC flux in a compact setup furthermore enables ground based mobile atom interferometers with a high repetition rate for geodesy applications.

The presented results of QUANTUS-2 were beating the previously fastest BEC machine operating at a 1 Hz repetition rate [109] by almost one order of magnitude in the achieved BEC atom number. The setup furthermore produces the largest condensates of all the experiments aiming at a fast BEC production. Astonishingly, the high flux of 2.5×10^5 atoms per second is also in the same range as of lab-filling BEC experiments. These setups usually rely on high power Zeeman slower for fast MOT loading in addition with high-intensity dipole traps for evaporative cooling and they produce large BECs of 10^7 atoms in tens of seconds. For a comparison, the results of QUANTUS-2 and other BEC setups are listed in table 3.1. While most of the setups are working with alkali metal atoms, e.g. Rb, K, Na, or Cs, due to the maturity of both the hardware technology and the atom optical methods there are some experiments using Sr or Yb atoms as an alternative candidate. These alkaline earth metal atoms offer more possibilities for cooling and manipulation but at the same time require setups with higher complexity and power consumption. The interesting properties of Sr and Yb paired with the recent progress in technology [115–120] put these as attractive candidates for large atomic fountains [24, 25, 121, 122] and future space missions [45, 123, 124].

Table 3.2: Comparison of source requirements. Achieved results of QUANTUS-2 in comparison with requirements for current and future projects. For BEC number and flux higher values are better, for expansion energy and velocity lower values are favourable.

project	BEC number 10^5	BEC flux $10^5/\text{s}$	expansion energy pK	expansion velocity $\mu\text{m/s}$
QUANTUS-2	4	2.5	38	50
STE-QUEST	10	1	50	80
CAI	10	10	50	80
BECCAL	10	10	50	80

With the excellent performance of QUANTUS-2, the setup established itself as a basis for proposals on future ground-based or space-borne atom interferometry applications. These projects range from the absolute gravity sensor for field applications QG-1 [125] to a test of the weak equivalence principle within the mission STE-QUEST [43], the gravity gradiometer CAI for satellite-based geodesy [65], or the multi-user facility BECCAL [126] for experiments with ultra-cold atoms on the International Space Station (ISS). The challenging requirements of these projects on the BEC source in terms of flux and expansion velocity are mostly matched by the results of QUANTUS-2 (see table 3.2). The required increase in performance could be achieved by further optimizing the atom-chip design, by improving the vacuum quality to reduce atom losses, or by utilizing enhanced control and driving electronics in the setup.

Currently, QUANTUS-2 is performing atom interferometry and will continue the coherence studies of QUANTUS-1 in the drop tower. With the faster BEC preparation time and the catapult mode it should be possible to extend the interferometry time to several seconds. Higher atom number and an improved detection system will also help to identify the reason for the loss of contrast experienced in QUANTUS-1. Eventually, QUANTUS-2 will be upgraded with the capabilities for cooling and manipulating K atoms to a two-species atom interferometer to perform tests of the weak equivalence principle in extended free fall in the drop tower.

CHAPTER 4

Atom interferometry in space

The promising results achieved with the QUANTUS-2 setup were decisive for the pursuit of bringing BEC-based atom interferometry into space. After successful operation in the drop tower, the sounding rocket mission MAIUS-1 was initiated as the next iteration towards an experiment on a dedicated satellite. During the parabolic flight the rocket payload reaches an altitude of 243 km and delivers a high-quality microgravity environment for six minutes. By crossing the Kármán line at a height of 100 km, a sounding rocket flight is also the first step into outer space. The main goal of the mission was to show the feasibility to create the first BEC in space and to demonstrate key atom-optic methods for high-precision atom interferometry in this microgravity environment.

The sounding rocket environment is quite different to the drop tower and brings new requirements and challenges along: The six minutes of microgravity are provided during one single run instead of being scattered on multiple drops spanning over several weeks or months. The shape and size of the experiment has to be adapted for aerodynamic reasons to a thinner but longer housing. New concepts for the power supply, the thermal management, and the data communication are required as the experiment has to operate independently for an extended time before, during, and after the flight. Additional implications on the design of the experiment stem from the increased accelerations, rotations, and vibrations experienced in the course of the sounding rocket flight, in particular on lift-off, during the spin-stabilized ascent, while re-entering into the atmosphere, and last but not least due to the impact on ground.

Based on the heritage of the QUANTUS-2 setup the follow-up BEC experiment MAIUS-A was designed and built (section 4.1) in accordance with all the requirements of the sounding rocket flight. To ensure the success of the mission, severe tests were conducted throughout the process. With a final test of the whole setup in operational conditions, the scientific payload was qualified for the use on a sounding rocket mission. Afterwards, the flight campaign (section 4.2) was prepared and conducted on the launch facility ESRANGE in Sweden during the winter of 2016/17. With the successful launch on the 23rd January 2017, the first BEC in space was created and studied for its application for space-borne precision atom interferometry.

This chapter describes the design and qualification of the scientific payload based on the requirements of a sounding rocket flight, the preparation and conduction of the MAIUS-1 flight campaign, and the most important experimental results. Further details and in-depth descriptions about the hardware, the tests and the campaign can be found in the corresponding dissertations of my colleagues [92, 127–131].

4.1 MAIUS-A: Design and qualification of scientific payload

The two-staged VSB-30 type sounding rocket [132] was selected as the appropriate launch vehicle for the MAIUS-1 mission because of its well-known and comparably low vibrational profile [133] given the supported payload size and mass and the provided microgravity time. The scientific payload MAIUS-A (see fig. 4.1) was designed to fit this vehicle and to fulfil all the requirements of the sounding rocket mission. The scientific payload consists of five interconnected modules containing the individual systems. The modules have a diameter of 0.5 m each and a total length of 2.8 m. The scientific payload has a resulting volume of 0.55 m³ and a total weight of 309 kg including the robust hull. Due to the new demands in stability and thermal management for the hull and supporting structure, it exceeds the size and mass of the QUANTUS-2 drop tower setup. The experiment draws an average power of about 300 W during operation. The setup is temperature stabilized by two individual water cooling systems while operating on ground. During the flight, the excess heat is stored in the thermal capacity of the aluminium supporting structure.

The experimental setup is based on the heritage of the drop tower experiments QUANTUS-1 and -2. The vacuum system contains a 2D-MOT for fast loading of the MOT and an atom-chip setup for the high-flux BEC production. The compact and robust laser system [56] consists of micro-integrated diode lasers, optical Zerodur benches [134], and fibre-based components. The electronic system is mostly based on in-house built electronic boards with digital FPGA (field-programmable gate array) circuits. A rugged computer with a custom developed software [135] is used to control the electronics and for communication with the ground control stations. The power supply of the payload is based on batteries and has advanced monitoring and switching capabilities.

Vacuum system

The vacuum system (fig. 4.1) is structured into two parts which are mounted on both sides of a common base plate and connected through a vacuum tube in the centre. The pumping system on the top side contains the vacuum pumps, an ion getter and a titanium sublimation pump, for maintaining the ultra-low pressure of below 10⁻¹⁰ mbar, a vacuum sensor for monitoring, and the electronics for data acquisition and switching. An additional battery allows the system to run independent from the main setup and thus to maintain the vacuum quality at all times. The bottom side is surrounded by a three-layer magnetic shield to block the experiment from external

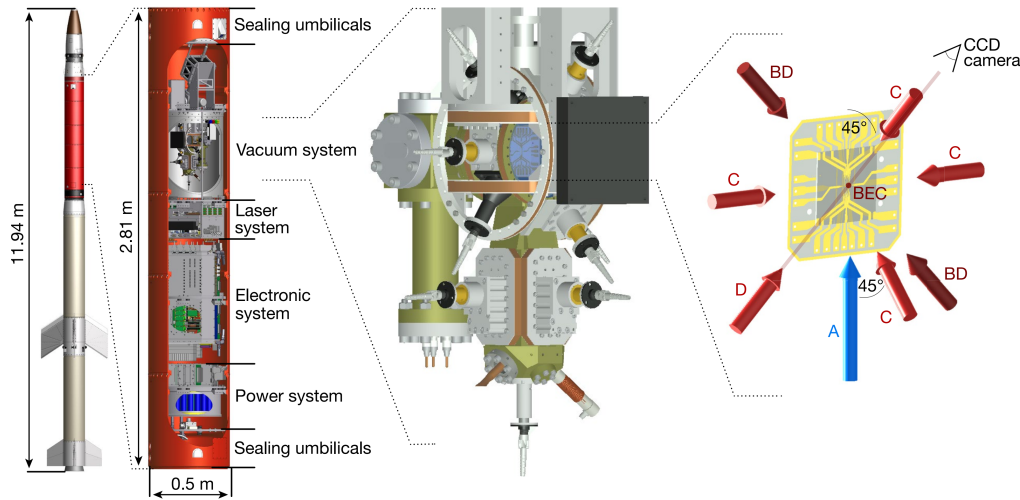


Figure 4.1: MAIUS-1 setup. From left to right: two-stage VSB-30 type sounding rocket, scientific payload MAIUS-A, vacuum system, and atom chip. A cold atomic beam (blue arrow A) loads the 3D-MOT generated by the 4 cooling laser beams (red arrows C) and the atom chip. Afterwards, the BEC is created in, transported by and released from the magnetic trap of the atom chip. The two counter-propagating light beams (BD) are utilized for Bragg diffraction. For detection of the BECs, a CCD camera images the absorption of the cold atoms using detection light (D). Adapted from [A4].

magnetic disturbances [136]. Inside the shield the two main vacuum chambers are situated: a high-pressure (10^{-7} mbar) source chamber to create the 2D-MOT and a low-pressure (10^{-10} mbar) science chamber to collect the atoms in a 3D-MOT, to produce the BEC, and to perform atom interferometry.

The source chamber has a temperature-stabilized oven containing 1 g of rubidium in natural abundance attached. The temperature of the oven influences the Rb background pressure inside the source chamber and is set at around 35°C for optimal operation. The magnetic coils for the quadrupole field are directly mounted onto the source chamber for a compact and robust setup. The source chamber is connected to the science chamber via a differential pumping stage including a graphite inlet. The science chamber has the three-layer atom chip installed inside. Additionally, three pairs of coils in Helmholtz configuration are mounted around the chamber. Together, these can create the trapping potentials for the MOT or the Ioffe-Pritchard trap [137] as well as homogeneous offset fields necessary for preparation and detection of the atoms. The atom chip furthermore contains several radio-frequency structures for evaporative cooling and state preparation.

The optic components to enlarge, collimate, and circular polarize the light coming via fibres from the laser system are directly attached to the two chambers to ensure

a stable alignment of the light beams. For the atom interferometry setup two of such collimators are used to create the counter-propagating light beams. To detect the atoms two imaging systems based on CCD (charge-coupled device) cameras are utilized. The absorption and the fluorescence detection system are orthogonal in respect to each other and to the interferometry axis to enable for an unobstructed image of the interferometry fringes.

Qualification process

Throughout the design phase and while setting up the experiment, a variety of tests were performed to ensure that all the requirements imposed by the sounding rocket mission are matched. At the beginning, these qualification tests involved vibration tests of single components, e.g. optical collimators, laser modules, or vacuum pumps, and later on of small subsystems, e.g. the atom-chip setup, an optical Zerodur bench, or the electronic module of the pumping system. The vibration tests were performed along the three main axes of the system and each consisted of three steps including a resonance sweep, a random noise test, and a final resonance sweep. The random noise tests are executed at different power levels depending on the tested setup: flight level at $2.0 \text{ g}_{\text{rms}}$, acceptance level at $5.4 \text{ g}_{\text{rms}}$, or qualification level at $8.1 \text{ g}_{\text{rms}}$.

This qualification process helped to select commercial components appropriate for the use on sounding rockets and to improve the overall design of the system in terms of robustness and stability. After all the chosen components and the built subsystems had been successfully qualified the main modules, e.g. electronic system or laser system, of the setup were constructed and tested for functionality. Afterwards, these systems had also to undergo vibration tests to check their performance. During these tests the systems were fully operational and the core parameters of each system were monitored. For the vacuum system the key parameter is the ultra-low vacuum pressure. During the vibrations induced by the launch the vacuum pressure is expected to rise significantly. The pumping system has to reduce the pressure level to be back below a certain threshold of $5 \times 10^{-10} \text{ mbar}$ to enable low losses of the cold atoms. The tests with the vacuum system have shown that it takes 40 s to reach the threshold on acceptance level and just 6 s on flight level [A3]. Both results are well below the limit of 60 s given by the time between the end of high vibrations during the acceleration phase and the beginning of the measurement phase in microgravity.

Finally, several tests including spinning of the payload to identify and compensate imbalances and another vibration test had to be performed with the complete scientific payload. These tests ensured that there are no safety risks and were required to qualify the payload for the launch on a sounding rocket. They furthermore assured that the functionality of the experiment is not affected by the conditions during the flight. To validate the experimental performance a set of representative measurements were executed before, during, and directly after the random vibration tests. The apparatus was able to consistently produce BECs of 1×10^5 atoms and to perform

BEC-based atom interferometry at a pulse separation time of $T = 2$ ms with a contrast of around 40 % both before and right after the induced vibrations.

4.2 MAIUS-1: Sounding rocket flight campaign

After the successful qualification of the payload for the sounding rocket, all the required hardware was brought to the launch facility Esrange Space Center [79] located in northern Sweden for the flight campaign MAIUS-1. This included the scientific payload MAIUS-A and the other payload modules from DLR-MORABA [138] to control and to communicate with the rocket as well as all the ground support equipment. This support equipment comprises the power supplies to operate on ground and charge the batteries of the payload, chillers for the water cooling system, several computers functioning as ground stations for monitoring and controlling both the experiment and the sounding rocket, and plenty of network components for data communication. The payload and all the ground stations were first set up in a separate hangar on the facility. Here, the procedure for the countdown was developed and intensively tested. Once the countdown procedure was established and the experiment was performing as specified the payload was brought to the launch tower while the ground stations were set up in a separate blockhouse for safety reasons. In this configuration the training of the countdown procedure was continued to establish a routine and to prepare for unexpected events. Furthermore, daily system and performance checks were conducted with the experiment to ensure an optimal performance for the flight. The reproducibility of the results demonstrated the stability of the system.

For a successful flight several conditions besides the experimental performance had to be fulfilled. External effects, e.g. strong winds or unsteady weather, can pose safety risks and had to be monitored constantly. To compensate for wind the launching angle could be tilted to adjust the flight trajectory. The different alignment of the payload influenced the performance of the experiment due to the changed orientation in respect to gravity. In a dedicated measurement the influence on the pointing of the launcher was analysed and thus could be taken into account during countdown. On the 23rd of January 2017 all the requirements were matched and the sounding rocket MAIUS-1 was successfully launched into space [A4]. The flight was nominal and the payload reached an altitude of 243 km providing six minutes of microgravity (see fig. 4.2). During the flight the alignment and the rotation rate of the payload was controlled by the onboard attitude and rate control system. The system first stabilized the payload after the rocket motors finished accelerating and were disconnected from it. During the drag-free parabolic flight the system was used twice to reduce any disturbing residual rotations or tilts of the scientific payload. After re-entry into the atmosphere the parachute opened and the payload landed on snow-covered ground about 60 km north of the launch facility. After the payload was

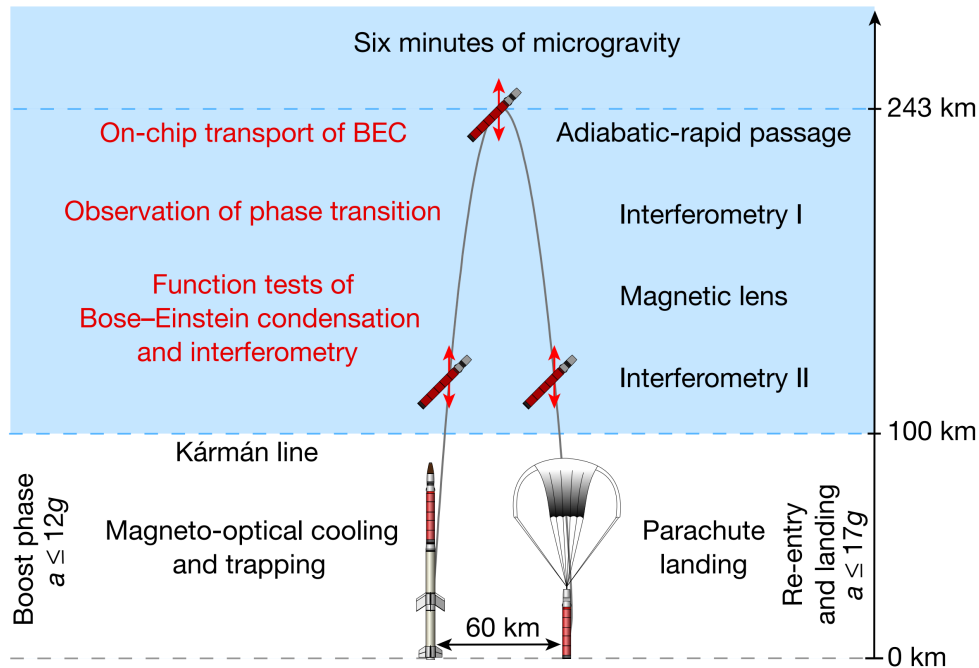


Figure 4.2: Flight schedule of MAIUS-1. The payload was accelerated with up to 12g and reached an altitude of 243 km. The parabolic space flight above 100 km provided 6 minutes of microgravity. During this time a variety of experiments grouped as measurement blocks were performed. The payload landed on a parachute about 60 km north of the launching facility. Taken from [A4].

brought back to the hangar on the launching facility it was thoroughly inspected for damages and the experimental data stored onboard was retrieved.

In the six minutes of microgravity a variety of atom optics experiments were performed [A4]. These measurements were grouped into several blocks each studying different aspects of BEC-based atom interferometry (see fig. 4.2). At the beginning a more general function test was conducted to ensure that all the hardware was working as expected. Afterwards the mostly predefined but still interactive measurement plan was carried out. Different to the experiments in the drop tower the microgravity time extends in one single run. This continuous manner leads to less deviations in between several measurement points or experiment blocks and makes it easier to correlate the results. As a drawback there is almost no time to evaluate and react to the experimental data. Typically, in-depth data evaluation leads to incremental changes in the measurement sequence or of single parameters and thus helps to obtain optimal results. For the sounding rocket mission a custom decision graph with automatic image and block evaluation was developed for the control of the experiment. The graph consisted of numerous predefined measurement blocks arranged in a decision

tree. Each block included a row of measurements points which were analysed individually at first. The evaluated result of the measurement block was then used to choose the next branch in the decision tree. With an additional downlink of compressed measurement data specific parameters or decisions could be controlled through a limited uplink from ground.

Space-borne BEC for precision interferometry

The main goal of the mission, the demonstration of the first Bose-Einstein condensate in space, was already achieved after a few seconds in microgravity during the function test at the beginning of the measurement plan. The initial performance of the system was as good as on ground and 10^5 condensed atoms were produced in about 1.6 seconds [A4]. Although implemented in the decision graph, further optimization, e.g. increasing the loading time of the MOT or adjusting offset fields of the magnetic trap, was neglected by the decision graph to utilize more microgravity time to extensively study the BEC. In particular, first the phase transition of the cold atoms into the BEC was analysed and following the evolution of the BEC both in the trap and during free fall was studied.

To study the phase transition into the BEC the final radio frequency of the forced evaporation was varied. This changes the temperature of the atomic ensemble and thus the fraction of condensed atoms. Comparing the results to previously obtained measurements on ground revealed two main differences: The measured BEC fraction was lower for the same applied radio frequency as on ground. This shift can be explained with a lowered trap bottom due to changes in the magnetic fields. Secondly, the atom number both in the thermal and in the condensed part was significantly higher than on ground. This improvement was probably caused by a more efficient loading of the atoms into the first magnetic trap due to the absence of the gravitational sag usually deforming the trapping potential on ground. Additionally, the low-noise environment during the space flight reduces the loss of atoms from the trap thus leading to a higher efficiency of the evaporative cooling. Adjusting key parameters of the experimental sequence to these circumstances could potentially further increase the overall atom number and the BEC fraction. These optimizations were omitted on this mission as they usually take longer than all the available time on this flight. However, a future orbital mission could greatly benefit from these findings to reach an even higher BEC flux. Here, only the final value of the radio frequency was adjusted to have a high BEC fraction for the following measurements during the flight.

One key method for performing precision atom interferometry with this kind of setup is the transport of the produced BEC further away from the surface of the atom chip. This is necessary to on the one hand allow the BEC to freely evolve over several seconds without expanding into the chip surface and on the other hand to reduce perturbing effects in the interferometry beams due to diffraction on the chip

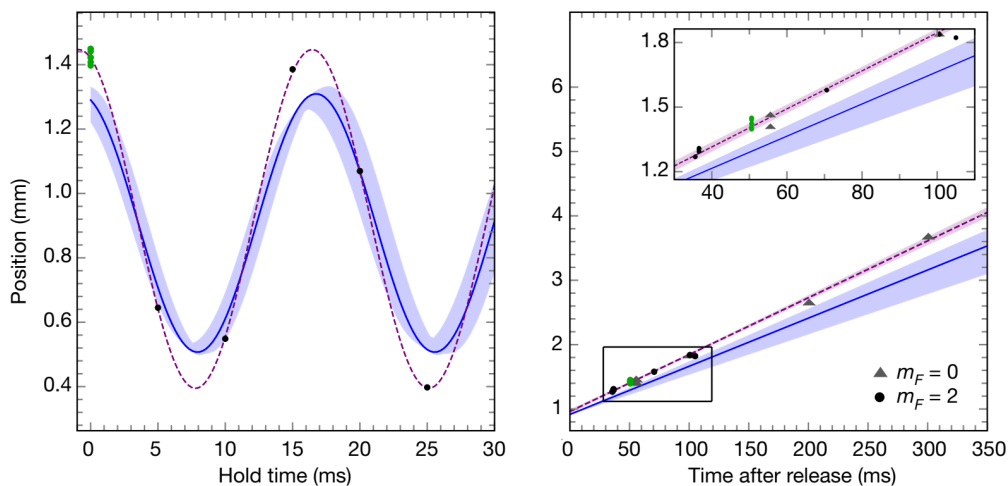


Figure 4.3: Excitation of the centre-of-mass motion and oscillations after transport. Oscillation in position for varying hold time detected after a time of flight of 50 ms (left). Free expansion of atoms directly released after transport (right). No significant difference for atoms in $|m_F = 2\rangle$ or $|m_F = 0\rangle$. Sinusoidal and linear fit to data as dashed line. Simulations including uncertainties as blue line and shaded areas. Adapted from [A4].

edge. The transport is realized by slowly changing the offset magnetic field which is displacing the trapping potential. Here, the atoms were moved with a 50 ms long sigmoidal ramp to a distance of about 1 mm away from the atom-chip surface. After a certain hold time the atoms were released from the trap and detected after 50 ms of free expansion. Altering the hold time allowed studying the temporal evolution of the atoms in the trap (see fig. 4.3). From the varying position of the atoms after the time of flight the oscillation in the trap coming from the transport can be calculated. The transport additionally induces complex coupled oscillations of the shape of the BEC in the trap. Although these shape oscillations are small they become clearly visible by the long free expansion of 50 ms before detection.

The experimental results were compared to simulated predictions based on a detailed model of the setup consisting of the atom chip and the magnetic coils. These simulations included measured or gauged uncertainties of the applied currents and of the geometric dimensions of the setup. The results of the simulations including the uncertainties in the current values are represented as the blue line with the shaded areas in figure 4.3. The measured data is in agreement with the simulations and the verification of the model was a crucial part for future atom-chip experiments.

Following the transport and the release, a state preparation was implemented to change the magnetic state of the atoms. During the transport the cold atoms are still in the magnetic susceptible $|m_F = 2\rangle$ state. Fluctuations in the magnetic

field would thus lead to large noise contributions in an atom interferometer. With an adiabatic rapid passage the atoms can be efficiently transferred into different Zeeman states and in particular into the non-magnetic state $|m_F = 0\rangle$ required for precision atom interferometry. Here, the atoms were transferred to a mixture of the $|m_F = 0\rangle$ and the two neighbouring $|m_F = \pm 1\rangle$ states. With the atoms being in this configuration it is possible to identify residual magnetic field gradients resulting in a relative displacement after time of flight. Based on the few conducted measurements the residual magnetic field gradients seem to be small or even negligible.

Furthermore, the free expansion of the BEC was studied over an extended free-fall time. For this, the atoms were released from the trap right after the transport and no extra hold time was added. The size and the position of the atomic cloud were detected after a time of flight of up to 300 ms (fig. 4.3). The harsh displacement of the trap during the transport induced a velocity onto the atoms of 8.8 mm/s. Due to the good control and the intrinsic stability of the atom-chip setup the relative fluctuations on the release velocity were as low as 1%. By utilizing advanced methods for the transport and the release, e.g. based on protocols of shortcut to adiabaticity [63, 105] or optimal control theory [106, 107], the fluctuations and also the amplitude itself can be further decreased which will be important for future atom interferometry experiments.

Ultracold atom interferometry in space

A variety of interference experiments with ultra-cold atoms were already conducted during the microgravity phase of the MAIUS-1 space flight. In these experiments both individual and sequences of Bragg light pulses were investigated [A5]. At first, the coherent population transfer for a single pulse was analysed regarding the Rabi detuning and the light intensity of the laser beams. Following, sequences of multiple pulses were utilized to perform a number of coherence experiments with the BECs. Within these experiments light-pulse interferometry together with phase imprinting were employed to investigate the spatial coherence of multiple spinor components of a BEC (fig. 4.4). In the observation of the interference patterns the microgravity environment was crucial to resolve the spatial coherence of the BECs and it was possible to measure differential forces acting on the various spinor components. This scheme could be utilized as a vector magnetometer in three dimensions or to precisely determine the position of the BEC as required for future satellite missions aiming to test the equivalence principle [43]. All these interference experiments performed during the MAIUS-1 flight open up the path towards high-precision atom interferometry in space.

Discussion of results

As part of the MAIUS-1 sounding rocket mission studies of the BEC phase transition and of the collective oscillations induced by the transport were conducted. The

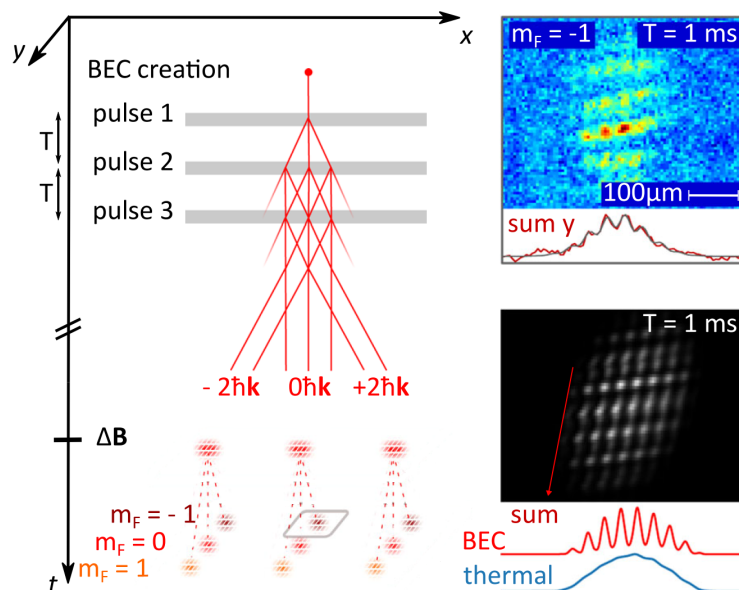


Figure 4.4: Shearing interferometer probing the spatial coherence of the different spinor components. Left: Interferometry sequence applied after the creation, transport, and release of the BEC consisting of three Bragg light pulses spaced by a pulse separation time T resulting in an interference pattern in the three output ports followed by a magnetic field gradient ΔB causing a Stern-Gerlach-type separation of the three different m_F -states. Top right: Interference pattern shown in the absorption image of an exemplary output port and in the corresponding line integral. Bottom right: Theoretical model based on the 2D-Gross-Pitaevskii equation of the BEC interacting with the interferometry light fields. Adapted from [A5].

demonstrated stability can be further improved by the implementation of more advanced transport protocols. This will enable future experiments to utilize the induced shape oscillations together with DKC to drastically reduce the expansion energy of the BEC. Reaching these ultra-low energies equivalent to a few picokelvins will allow for BEC-based precision atom interferometry in space on extended time scales of many seconds.

The achieved performance of the system in terms of the BEC atom number and flux are comparable to the results of the predecessor experiment QUANTUS-2 [A2]. This is in accordance to the expectations as the two experimental setups are very similar in design and specifications. The stability of the transport of the atoms on the atom chip shown during the flight is in the same range as the one obtained in the drop tower by QUANTUS-2. This allows adapting protocols for transport, release, and DKC from one system to the other. Thorough calibration of the hardware specification and in-depth verification of the atom-chip model are essential for the

successful implementation of these complex protocols.

On the MAIUS-1 mission the first Bose-Einstein condensation in space was realized. Around four months before that the Chinese CACES (Cold Atom Clock Experiment in Space) mission was launched and put into operation in orbit [139]. Here, laser cooled Rubidium atoms at low temperatures of a few μK are interrogated with microwave pulses to operate an atomic clock. Deploying these cold-atom clocks in space is foreseen to have improvements on various applications, e.g. the time keeping systems on Earth, the global navigation satellite system, or deep space tests of fundamental physics. The operation of CACES in orbit represents a milestone for cold-atom sensors in space. The experimental setup nevertheless does not allow to produce ultra-cold BECs and perform light-pulse atom interferometry.

Driven by the promising results of the QUANTUS collaboration the NASA initiated the CAL (Cold Atom Lab) project in the year 2012 [140]. The goal of the project was set to bring an experiment operating with ultra-cold atoms to the International Space Station. The experimental setup was built by the JPL and was based mainly on commercially available components to reduce the required time for developing and manufacturing. The CAL payload was launched and successfully installed on the ISS in May 2018. After a few months of operation involving trouble-shooting and experimental optimization the first BEC in orbit was realized in December 2018 [141]. As the experiment was based on a commercial setup the BEC performance of CAL with a total atom number of 4.9×10^4 and a condensate fraction of 26 % was slightly lower compared to the presented numbers achieved with the atom-chip setup employed in QUANTUS and MAIUS. The CAL setup was since used as a multi-user facility enabling various investigators to perform experiments with ultra-cold atoms in space [142–144]. Among others, a consortium including parts of the QUANTUS collaboration conducts transport and expansion studies similar to the ones performed by QUANTUS-2 and MAIUS-1. In May 2020, CAL performed atom interferometry with an ultracold BEC of rubidium atoms after the setup received an on-orbit upgrade of a new science module with atom interferometry capabilities [145].

Besides the here presented experiments the MAIUS-1 campaign led to additional important results: The MAIUS-A payload proved to be very stable and robust and was able to operate at a state-of-the-art performance in various different environments. With this setup it was possible to operate MOT experiments during the launch despite the large vibrations, accelerations, and rotations acting on the apparatus [131]. Here, the efficiency of first releasing the atoms from the MOT and then recapturing them after a certain time was analysed. The results are of wide interest as this approach could be implemented for high repetition rate atom interferometry in dynamic environments.

CHAPTER 5

Conclusion

In this thesis the important milestones of the QUANTUS collaboration to bring BEC-based atom interferometry from ground to space are presented. The QUANTUS-1 apparatus initiated the field of ultra-cold atoms in microgravity with the realization of the first BEC in free fall in the drop tower. The implementation of the DKC technique allowed studying the BEC of ten thousands of atoms for free expansion times of up to two seconds. Together the low expansion velocity and the high coherence of the BEC enabled performing Bragg-diffraction interferometry over extended free-fall times of 0.7 s. In the applied asymmetric Mach-Zehnder type interferometer both the spatial coherence and the contrast can be evaluated in a single shot measurement. For the follow-up drop tower experiment QUANTUS-2, an improved atom-chip setup was developed to realize a high-flux source for precision atom interferometry. The apparatus produced BECs of 4×10^5 atoms in 1.6 s resulting in the highest flux achieved for mobile BEC setups. The high flux of 10^5 atoms/s allowed QUANTUS-2 to extensively study the evolution of the BEC during free fall in the drop tower. The good performance in combination with the high reproducibility of the atom-chip setup enabled the implementation of advanced protocols for the transport and the release of the atoms as well as for the DKC. The protocols were developed and further optimized by theory simulations based on a comprehensive atom-chip model. With the excellent control of the BEC on the atom chip, a stability in position on the micrometer level and expansion velocities corresponding to tens of picokelvins were reached.

Driven by the success of the two drop tower experiments the scientific payload MAIUS-A was designed to operate on a sounding rocket mission and to realize the first BEC in space. The system was based on the atom-chip setup of QUANTUS-2 but required an improved level of all hardware components for the new challenging environment. Rigorous qualification and verification of the setup were carried out to guarantee the operation in the harsh environment of a sounding rocket flight. In the end, the system was able to produce BECs of 10^5 atoms in 1.6 s and to perform atom interferometry experiments using Bragg-diffraction light pulses. The implementation of a decision-tree-based sequence graph enabled the system to operate autonomously including the optimization of key parameters for evaporation or Bragg

diffraction. The high BEC flux, together with the sequence graph, allowed performing numerous measurements during the six-minute-long space flight of MAIUS-1. The phase transition into the BEC was analysed and the BECs were studied as a source for high-precision atom interferometry. Furthermore, a variety of experiments on Bragg-diffraction investigating the coherence of the BEC were conducted. The successful sounding rocket mission MAIUS-1 represents an important milestone for high-precision atom interferometry with BECs in space.

Outlook

The results presented in this manuscript, achieved with the drop tower experiments and on the sounding rocket mission, are the basis for various proposals on future atom interferometry experiments in space. The experience and knowledge gathered during the MAIUS-1 campaign will be especially helpful for the follow-on sounding rocket missions MAIUS-2 and MAIUS-3 [146]. The goal of these two campaigns is the development of the hardware technology and the demonstration of the atom optics methods for two-species differential atom interferometry. The new scientific payload MAIUS-B for these two flights will be capable of producing BECs of Rb-87 and K-41 and to perform dual-species atom interferometry. The new payload will be substantially upgraded to still fit the more advanced experiment on the same type of sounding rocket as the predecessor. For this, a new generation laser system capable of cooling and manipulating both species will be implemented. The electronic system will be further improved based on the lessons learned from the MAIUS-1 mission. The power supply concept will be optimized for the sounding rocket flight. Additional hardware components will be implemented for the simultaneous manipulation of the two species. These include a microwave antenna for the sympathetic evaporative cooling, a strong magnetic coil to be able to tune the interspecies scattering properties, and an optical dipole trap to study the mixture of the two species.

So far, most of the hardware was already built, assembled, and tested. In the lab, the MAIUS-B atom-chip setup is producing BECs with 3.5×10^5 Rb and 7×10^4 K atoms [147]. Next, all the necessary steps to perform Raman double-diffraction interferometry [148] will be implemented. This interferometry scheme is well suited for BEC-based dual-species measurements and has already been studied by the QUANTUS-1 experiment on ground. Once the interferometer is in operation and all the modules are finished, the system will be integrated in the hull structure for the sounding rocket flight. After a qualification of the complete payload it will be sent to Esrange Space Center in Sweden for launch preparation. On the two campaigns MAIUS-2 and -3 the key methods for two-species differential atom interferometry will be demonstrated which will pave the way for future tests of the weak equivalence principle in space.

Both the drop tower experiments and the sounding rocket flights are excellent test-beds for future space missions operating BEC-based atom interferometers in orbit.

With the recently built active drop tower Einstein-Elevator [77], a new facility will be available for experiments on ultra-cold atoms in microgravity. The elevator provides a microgravity time of four seconds and allows for up to 300 launches per day. The flight capsule has inner dimensions of $\varnothing 1.7\text{ m} \times 2\text{ m}$ and the tower supports payloads of up to 1000 kg. These generous specifications enable the easy implementation of various setups and especially of the MAIUS payloads. In particular, one proposal plans to utilize the MAIUS-A setup in the drop tower to conduct searches of dark matter and dark energy [149]. To this end, a specially designed interferometry chamber would be attached to the science chamber to maximize the sensitivity of the measurement. For the MAIUS-B experiment, the Einstein-Elevator can be very helpful for the success of the sounding rocket mission. It can be utilized beforehand to test and optimize the sequences and parameters for the flight and afterwards to verify some of the results or for potential failure investigation. The Einstein-Elevator will also be of great interest to test and optimize payloads for future missions continuously performing experiments in space.

One of these space missions will be the NASA-DLR collaboration BECCAL (Bose-Einstein Condensate and Cold Atom Laboratory) operating on the ISS [126]. The apparatus is planned to replace the CAL experiment and will also serve as a multi-user facility for experiments with ultra-cold atoms in the microgravity environment onboard the ISS. The BECCAL payload will be based on the MAIUS-B setup and will have the capabilities for cooling and manipulating the bosonic isotopes Rb-85, Rb-87, K-39, and K-41 as well as the fermionic K-40. The setup will include various additional components for preparation, trapping, and manipulation of the ultra-cold atoms. The excellent performing atom-chip setup in combination with all the new features will enable experiments on atom interferometry, coherent atom optics, scalar and spinor BECs or quantum gas mixtures, strongly interacting gases and molecules, and quantum information. The project is currently at the end of the design phase after which the construction and assembly of the apparatus will start. The launch into orbit is anticipated for the year 2024 and the payload is designed to operate for a mission duration of three years. With the ground-breaking experiments that can be performed with the BECCAL apparatus it will also serve as a pathfinder for proposals on dedicated satellite missions.

Two of such future satellite missions are already in the planning phase. The first one is the STE-QUEST mission aiming to perform a quantum test of the weak equivalence principle in space [43]. For this a dual-species interferometer operating with Rb-87 and K-41 analogue to the MAIUS-B experiment will be set up as a satellite payload. The second one, CAI, is a space gravity gradiometer based on cold-atom interferometry to map the Earth's gravitational field [65]. The instrument is based on the QUANTUS atom-chip setup with an additional separate interferometry chamber. The setup enables high-sensitivity measurements of gravity gradients by using multiple atom interferometers in a differential configuration. The presented

results of this thesis have set the basis for these two as well as other future proposals and the steady progress of the current projects will further increase the chances for the successful realization of these ambitious missions aiming at performing high-precision atom interferometry in space.

Bibliography

1. B. P. Abbott, R. Abbott, T. D. Abbott, M. R. Abernathy, F. Acernese, et al.: ‘Observation of Gravitational Waves from a Binary Black Hole Merger’. *Phys. Rev. Lett.* (6 Feb. 2016), vol. 116: p. 061102 (cit. on p. 1).
2. B. P. Abbott, R. Abbott, T. D. Abbott, F. Acernese, K. Ackley, et al.: ‘GW170817: Observation of Gravitational Waves from a Binary Neutron Star Inspiral’. *Phys. Rev. Lett.* (16 Oct. 2017), vol. 119: p. 161101 (cit. on p. 1).
3. K. U. Schreiber, T. Klügel, A. Velikoseltsev, W. Schlüter, G. Stedman, et al.: ‘The large ring laser G for continuous Earth rotation monitoring’. *Pure and applied geophysics* (2009), vol. 166(8-9): pp. 1485–1498 (cit. on p. 1).
4. L. de Broglie: ‘Recherches sur la théorie des Quantas’. Doktorarbeit. Universität von Paris, 1924 (cit. on p. 1).
5. E. L. Raab, M. Prentiss, A. Cable, S. Chu, and D. E. Pritchard: ‘Trapping of Neutral Sodium Atoms with Radiation Pressure’. *Phys. Rev. Lett.* (1987), vol. 59: pp. 2631–2634 (cit. on p. 1).
6. W. D. Phillips: ‘Nobel Lecture: Laser cooling and trapping of neutral atoms’. *Rev. Mod. Phys.* (3 1998), vol. 70: pp. 721–741 (cit. on p. 1).
7. P. R. Berman: *Atom Interferometry*. Academic Press, 1997 (cit. on p. 1).
8. M. Kasevich and S. Chu: ‘Atomic interferometry using stimulated Raman transitions’. *Phys. Rev. Lett.* (1991), vol. 67: pp. 181–184 (cit. on p. 1).
9. J. B. Fixler, G. T. Foster, J. M. McGuirk, and M. A. Kasevich: ‘Atom Interferometer Measurement of the Newtonian Constant of Gravity’. *Science* (2007), vol. 315: p. 74 (cit. on p. 1).
10. G. Rosi, F. Sorrentino, L. Cacciapuoti, M. Prevedelli, and G. Tino: ‘Precision measurement of the Newtonian gravitational constant using cold atoms’. *Nature* (2014), vol. 510(7506): pp. 518–521 (cit. on p. 1).
11. R. Bouchendir, P. Cladé, S. Guellati-Khélifa, F. Nez, and F. Biraben: ‘New determination of the fine structure constant and test of the quantum electrodynamics’. *Physical Review Letters* (2011), vol. 106(8): p. 080801 (cit. on p. 1).

12. R. H. Parker, C. Yu, W. Zhong, B. Estey, and H. Müller: ‘Measurement of the fine-structure constant as a test of the Standard Model’. *Science* (2018), vol. 360(6385): pp. 191–195 (cit. on p. 1).
13. S. Fray, C. A. Diez, T. W. Hänsch, and M. Weitz: ‘Atomic Interferometer with Amplitude Gratings of Light and Its Applications to Atom Based Tests of the Equivalence Principle’. *Phys. Rev. Lett.* (24 Dec. 2004), vol. 93: p. 240404 (cit. on p. 1).
14. D. Schlippert, J. Hartwig, H. Albers, L. L. Richardson, C. Schubert, et al.: ‘Quantum test of the universality of free fall’. *Physical Review Letters* (2014), vol. 112(20): p. 203002 (cit. on p. 1).
15. M. G. Tarallo, T. Mazzoni, N. Poli, D. V. Sutyryn, X. Zhang, et al.: ‘Test of Einstein Equivalence Principle for 0-Spin and Half-Integer-Spin Atoms: Search for Spin-Gravity Coupling Effects’. *Physical Review Letters* (July 2014), vol. 113(2), 023005: p. 023005 (cit. on p. 1).
16. L. Zhou, S. Long, B. Tang, X. Chen, F. Gao, et al.: ‘Test of Equivalence Principle at 10^{-8} Level by a Dual-Species Double-Diffraction Raman Atom Interferometer’. *Physical review letters* (2015), vol. 115(1): p. 013004 (cit. on p. 1).
17. G. Rosi, G. D’Amico, L. Cacciapuoti, F. Sorrentino, M. Prevedelli, et al.: ‘Quantum test of the equivalence principle for atoms in coherent superposition of internal energy states’. *Nature communications* (2017), vol. 8: p. 15529 (cit. on p. 1).
18. H. Albers, A. Herbst, L. L. Richardson, H. Heine, D. Nath, et al.: ‘Quantum test of the Universality of Free Fall using rubidium and potassium’. *The European Physical Journal D* (2020), vol. 74(7): pp. 1–9 (cit. on p. 1).
19. S. Hawking: *The theory of everything*. Jaico Publishing House, 2006 (cit. on p. 1).
20. A. Einstein: ‘Die Grundlage der allgemeinen Relativitätstheorie’. *Annalen der Physik* (1916), vol. 354(7): pp. 769–822 (cit. on p. 1).
21. S. Dimopoulos, P. W. Graham, J. M. Hogan, and M. A. Kasevich: ‘Testing General Relativity with Atom Interferometry’. *Phys. Rev. Lett.* (11 Mar. 2007), vol. 98: p. 111102 (cit. on p. 1).
22. J. M. Hogan, D. M. Johnson, S. Dickerson, T. Kovachy, A. Sugarbaker, et al.: ‘An atomic gravitational wave interferometric sensor in low earth orbit (AGIS-LEO)’. *General Relativity and Gravitation* (2011), vol. 43(7): pp. 1953–2009 (cit. on p. 1).

23. P. W. Graham, J. M. Hogan, M. A. Kasevich, S. Rajendran, and R. W. Romani: *Mid-band gravitational wave detection with precision atomic sensors*. 2017 (cit. on p. 1).
24. B. Canuel, A. Bertoldi, L. Amand, E. P. Di Borgo, T. Chantrait, et al.: ‘Exploring gravity with the MIGA large scale atom interferometer’. *Scientific reports* (2018), vol. 8(1): pp. 1–23 (cit. on pp. 1, 18).
25. B. Canuel, S. Abend, P. Amaro-Seoane, F. Badaracco, Q. Beaufiles, et al.: ‘ELGAR—a European laboratory for gravitation and atom-interferometric research’. *Classical and Quantum Gravity* (2020), vol. 37(22): p. 225017 (cit. on pp. 1, 18).
26. Y. A. El-Neaj, C. Alpigiani, S. Amairi-Pyka, H. Araujo, A. Balaz, et al.: *AEDGE: Atomic Experiment for Dark Matter and Gravity Exploration in Space*. 2019 (cit. on p. 1).
27. P. Cheiney, L. Fouché, S. Templier, F. Napolitano, B. Battelier, et al.: ‘Navigation-Compatible Hybrid Quantum Accelerometer Using a Kalman Filter’. *Phys. Rev. Applied* (Sept. 2018), vol. 10: p. 034030 (cit. on p. 1).
28. T. Gustavson, P. Bouyer, and M. Kasevich: ‘Precision rotation measurements with an atom interferometer gyroscope’. *Physical Review Letters* (1997), vol. 78(11): p. 2046 (cit. on p. 1).
29. A. Gauguier, B. Canuel, T. Lévêque, W. Chaibi, and A. Landragin: ‘Characterization and limits of a cold-atom Sagnac interferometer’. *Physical Review A* (2009), vol. 80(6): p. 063604 (cit. on p. 1).
30. P. Berg, S. Abend, G. Tackmann, C. Schubert, E. Giese, et al.: ‘Composite-light-pulse technique for high-precision atom interferometry’. *Physical review letters* (2015), vol. 114(6): p. 063002 (cit. on p. 1).
31. A. Peters, K. Y. Chung, and S. Chu: ‘Measurement of gravitational acceleration by dropping atoms’. *Nature* (Aug. 1999), vol. 400: pp. 849–852 (cit. on p. 1).
32. J. E. Debs, P. A. Altin, T. H. Barter, D. Döring, G. R. Dennis, et al.: ‘Cold-atom gravimetry with a Bose-Einstein condensate’. *Phys. Rev. A* (3 Sept. 2011), vol. 84: p. 033610 (cit. on p. 1).
33. Z.-K. Hu, B.-L. Sun, X.-C. Duan, M.-K. Zhou, L.-L. Chen, et al.: ‘Demonstration of an ultrahigh-sensitivity atom-interferometry absolute gravimeter’. *Phys. Rev. A* (4 2013), vol. 88: p. 043610 (cit. on p. 1).

34. C. Freier, M. Hauth, V. Schkolnik, B. Leykauf, M. Schilling, et al.: ‘Mobile quantum gravity sensor with unprecedented stability’. *Journal of Physics: Conference Series, 8th Symposium on Frequency Standards and Metrology 2015 12–16 October 2015, Potsdam, Germany* (2016), vol. 723: p. 012050 (cit. on pp. 1, 7).
35. V. Ménotet, P. Vermeulen, N. Le Moigne, S. Bonvalot, P. Bouyer, et al.: ‘Gravity measurements below 10^{-9} g with a transportable absolute quantum gravimeter’. *Scientific Reports* (2018), vol. 8(1): p. 12300 (cit. on p. 1).
36. X. Wu, Z. Pagel, B. S. Malek, T. H. Nguyen, F. Zi, et al.: ‘Gravity surveys using a mobile atom interferometer’. *Science advances* (2019), vol. 5(9): eaax0800 (cit. on p. 1).
37. M. Snadden, J. McGuirk, P. Bouyer, K. Haritos, and M. Kasevich: ‘Measurement of the Earth’s gravity gradient with an atom interferometer-based gravity gradiometer’. *Physical review letters* (1998), vol. 81(5): p. 971 (cit. on p. 1).
38. J. M. McGuirk, G. Foster, J. Fixler, M. Snadden, and M. Kasevich: ‘Sensitive absolute-gravity gradiometry using atom interferometry’. *Physical Review A* (2002), vol. 65(3): p. 033608 (cit. on p. 1).
39. J. Hartwig, S. Abend, C. Schubert, D. Schlippert, H. Ahlers, et al.: ‘Testing the universality of free fall with rubidium and ytterbium in a very large baseline atom interferometer’. *New Journal of Physics* (2015), vol. 17(3): p. 035011 (cit. on pp. 1, 7).
40. P. Asenbaum, C. Overstreet, M. Kim, J. Curti, and M. A. Kasevich: ‘Atom-Interferometric Test of the Equivalence Principle at the 10^{-12} Level’. *Phys. Rev. Lett.* (19 Nov. 2020), vol. 125: p. 191101 (cit. on pp. 1, 7, 14).
41. H. Müntinga, H. Ahlers, M. Krutzik, A. Wenzlawski, S. Arnold, et al.: ‘Interferometry with Bose-Einstein condensates in microgravity’. *Physical review letters* (2013), vol. 110(9): p. 093602 (cit. on p. 1).
42. B. Barrett, L. Antoni-Micollier, L. Chichet, B. Battelier, T. Lévèque, et al.: ‘Dual matter-wave inertial sensors in weightlessness’. *Nature Communications* (2016), vol. 7: p. 13786 (cit. on p. 1).
43. D. N. Aguilera, H. Ahlers, B. B Battelier, A. A Bawamia, A. Bertoldi, et al.: ‘STE-QUEST — test of the universality of free fall using cold atom interferometry’. *Classical and Quantum Gravity* (2014), vol. 31(11): p. 115010 (cit. on pp. 1, 2, 19, 29, 35).
44. O. Carraz, C. Siemes, L. Massotti, R. Haagmans, and P. Silvestrin: ‘A Spaceborne Gravity Gradiometer Concept Based on Cold Atom Interferometers for Measuring Earth’s Gravity Field’. *Microgravity Science and Technology* (2014), vol. 26(3): pp. 139–145 (cit. on p. 1).

45. G. M. Tino, A. Bassi, G. Bianco, K. Bongs, P. Bouyer, et al.: ‘SAGE: A proposal for a space atomic gravity explorer’. *The European Physical Journal D* (Nov. 2019), vol. 73(11): p. 228 (cit. on pp. 1, 18).
46. S. Bose: ‘Plancks Gesetz und Lichtquantenhypothese’. *Zeitschrift für Physik* (1924), vol. 26: pp. 178–181 (cit. on pp. 1, 9).
47. A. Einstein: ‘Quantentheorie des einatomigen idealen Gases’. *Sitzungsber. Kgl. Preuss. Akad. Wiss.* (1924), vol. 1924: p. 261 (cit. on pp. 1, 9).
48. K. B. Davis, M. -.-O. Mewes, M. R. Andrews, N. J. van Druten, D. S. Durfee, et al.: ‘Bose-Einstein Condensation in a Gas of Sodium Atoms’. *Phys. Rev. Lett.* (1995), vol. 75: pp. 3969–3973 (cit. on pp. 1, 9).
49. M. H. Anderson, J. R. Ensher, M. R. Matthews, C. E. Wieman, and E. A. Cornell: ‘Observation of Bose-Einstein Condensation in a Dilute Atomic Vapor’. *Science* (1995), vol. 269: pp. 198–201 (cit. on pp. 1, 9).
50. E. A. Cornell and C. E. Wieman: ‘Nobel Lecture: Bose-Einstein condensation in a dilute gas, the first 70 years and some recent experiments’. *Reviews of Modern Physics* (2002), vol. 74(3): p. 875 (cit. on pp. 1, 9).
51. W. Ketterle: ‘Nobel lecture: When atoms behave as waves: Bose-Einstein condensation and the atom laser’. *Rev. Mod. Phys.* (4 Nov. 2002), vol. 74: pp. 1131–1151 (cit. on pp. 1, 9).
52. S. Chu, J. Bjorkholm, A. Ashkin, and A. Cable: ‘Experimental observation of optically trapped atoms’. *Physical review letters* (1986), vol. 57(3): p. 314 (cit. on p. 1).
53. T. Kovachy, J. Hogan, A. Sugarbaker, S. Dickerson, C. Donnelly, et al.: ‘Matter Wave Lensing to Picokelvin Temperatures’. *Phys. Rev. Lett.* (2015), vol. 114: p. 143004 (cit. on p. 1).
54. K. Bongs, M. Holynski, J. Vovrosh, P. Bouyer, G. Condon, et al.: ‘Taking atom interferometric quantum sensors from the laboratory to real-world applications’. *Nature Reviews Physics* (Oct. 2019), vol. 1: p. 731 (cit. on p. 2).
55. M. Schiemangk et al.: ‘High-power, micro-integrated diode laser modules at 767 and 780 nm for portable quantum gas experiments’. *Appl. Opt.* (June 2015), vol. 54(17): pp. 5332–5338 (cit. on p. 2).
56. V. Schkolnik, O. Hellmig, A. Wenzlawski, J. Grosse, A. Kohfeldt, et al.: ‘A compact and robust diode laser system for atom interferometry on a sounding rocket’. *Applied Physics B* (July 2016), vol. 122(8): p. 217 (cit. on pp. 2, 22).
57. W. Hänsel, P. Hommelhoff, T. W. Hänsch, and J. Reichel: ‘Bose–Einstein condensation on a microelectronic chip’. *Nature* (2001), vol. 413: pp. 498–501 (cit. on p. 2).

58. R. Folman, P. Krüger, J. Schmiedmayer, J. Denschlag, and C. Henkel: ‘Microscopic atom optics: from wires to an atom chip’. *Adv. At., Mol., Opt. Phys.* (2002), vol. 48: p. 263 (cit. on p. 2).
59. J. Fortágh and C. Zimmermann: ‘Magnetic microtraps for ultracold atoms’. *Rev. Mod. Phys.* (1 Feb. 2007), vol. 79: pp. 235–289 (cit. on p. 2).
60. T. van Zoest, N. Gaaloul, Y. Singh, H. Ahlers, W. Herr, et al.: ‘Bose-Einstein condensation in microgravity’. *Science* (2010), vol. 328(5985): pp. 1540–1543 (cit. on pp. 2, 11, 12).
61. D. Becker, M. D. Lachmann, S. T. Seidel, H. Ahlers, A. N. Dinkelaker, et al.: ‘Space-borne Bose-Einstein condensation for precision interferometry’. *Nature* (7727 2018), vol. 562: pp. 391–395 (cit. on p. 2).
62. H. Ahlers, H. Müntinga, A. Wenzlawski, M. Krutzik, G. Tackmann, et al.: ‘Double Bragg Interferometry’. *Phys. Rev. Lett.* (17 Apr. 2016), vol. 116: p. 173601 (cit. on p. 2).
63. R. Corgier, S. Amri, W. Herr, H. Ahlers, J. Rudolph, et al.: ‘Fast manipulation of Bose-Einstein condensates with an atom chip’. *New Journal of Physics* (2018), vol. 20(5): p. 055002 (cit. on pp. 2, 17, 29).
64. R. Corgier, S. Loriani, H. Ahlers, K. Posso-Trujillo, C. Schubert, et al.: ‘Interacting quantum mixtures for precision atom interferometry’. *New Journal of Physics* (2020), vol. 22(12): p. 123008 (cit. on p. 2).
65. A. Trimeche, B. Battelier, D. Becker, A. Bertoldi, P. Bouyer, et al.: ‘Concept study and preliminary design of a cold atom interferometer for space gravity gradiometry’. *Classical and Quantum Gravity* (2019), vol. 36(21): p. 215004 (cit. on pp. 2, 19, 35).
66. P. J. Martin, B. G. Oldaker, A. H. Miklich, and D. E. Pritchard: ‘Bragg scattering of atoms from a standing light wave’. *Physical review letters* (1988), vol. 60(6): p. 515 (cit. on p. 5).
67. E. M. Rasel, M. K. Oberthaler, H. Batelaan, J. Schmiedmayer, and A. Zeilinger: ‘Atom wave interferometry with diffraction gratings of light’. *Physical Review Letters* (1995), vol. 75(14): p. 2633 (cit. on p. 5).
68. C. J. Bordé: ‘Atomic interferometry with internal state labelling’. *Physics letters A* (1989), vol. 140(1-2): pp. 10–12 (cit. on p. 5).
69. M. Kasevich and S. Chu: ‘Atomic interferometry using stimulated Raman transitions’. *Physical review letters* (1991), vol. 67(2): p. 181 (cit. on p. 5).
70. T. L. Gustavson, P. Bouyer, and M. A. Kasevich: ‘Precision Rotation Measurements with an Atom Interferometer Gyroscope’. *Phys. Rev. Lett.* (1997), vol. 78: pp. 2046–2049 (cit. on p. 5).

71. M. Kasevich and S. Chu: ‘Measurement of the gravitational acceleration of an atom with a light-pulse atom interferometer’. *Applied Physics B* (1992), vol. 54(5): pp. 321–332 (cit. on p. 5).
72. F. Riehle, T. Kisters, A. Witte, J. Helmcke, and C. J. Bordé: ‘Optical Ramsey spectroscopy in a rotating frame: Sagnac effect in a matter-wave interferometer’. *Physical review letters* (1991), vol. 67(2): p. 177 (cit. on p. 6).
73. O. Carnal and J. Mlynek: ‘Young’s double-slit experiment with atoms: A simple atom interferometer’. *Physical review letters* (1991), vol. 66(21): p. 2689 (cit. on p. 6).
74. H. Müntinga: ‘Matter-wave Interferometry for space-borne Inertial Sensors’. Dissertation. Universität Bremen, 2019 (cit. on pp. 7, 12).
75. T. Kovachy, P. Asenbaum, C. Overstreet, C. A. Donnelly, S. M. Dickerson, et al.: ‘Quantum superposition at the half-metre scale’. *Nature* (Dec. 2015), vol. 528(7583): pp. 530–533 (cit. on pp. 7, 14).
76. *ZARM Drop Tower Bremen User Manual*, <https://www.zarm.uni-bremen.de/en/drop-tower/experiment-support.html>. Drop Tower Operation and Service Company ZARM FABmbH. 2012 (cit. on pp. 8, 11).
77. C. Lotz, T. Froböse, A. Wanner, L. Overmeyer, and W. Ertmer: ‘Einstein-Elevator: A New Facility for Research from μg to 5 g’. *Gravitational and Space Research* (2017), vol. 5(2) (cit. on pp. 8, 35).
78. Novespace and A. Z. G: *Scientific research flights*. <https://www.airzerog.com/scientific-research-services/> (cit. on pp. 8, 14).
79. Swedish Space Corporation: *Science and launch services - Sounding rockets*. <https://sscspace.com/services/science-and-launch-services/sounding-rockets/> (cit. on pp. 8, 25).
80. J. Dalibard and C. Cohen-Tannoudji: ‘Laser cooling below the Doppler limit by polarization gradients: simple theoretical models’. *J. Opt. Soc. Am. B* (11 1989), vol. 6: pp. 2023–2045 (cit. on p. 8).
81. K. W. Madison, F. Chevy, W. Wohlleben, and J. Dalibard: ‘Vortex formation in a stirred Bose-Einstein condensate’. *Physical review letters* (2000), vol. 84(5): p. 806 (cit. on p. 9).
82. T. Hensel, S. Loriani, C. Schubert, F. Fitzek, S. Abend, et al.: ‘Inertial sensing with quantum gases: a comparative performance study of condensed versus thermal sources for atom interferometry’. *The European Physical Journal D* (2021), vol. 75(3): pp. 1–13 (cit. on p. 9).

83. J. Rudolph, N. Gaaloul, Y. Singh, H. Ahlers, W. Herr, et al.: ‘Degenerate Quantum Gases in Microgravity’. *Microgravity Science and Technology* (3 2011), vol. 23: pp. 287–292 (cit. on p. 12).
84. T. van Zoest: ‘Realisierung erster quantenentarteter Gase unter Schwerelosigkeit’. Dissertation. Institut für Quantenoptik, Leibniz Universität Hannover, 2008 (cit. on p. 12).
85. W. Herr: ‘Eine kompakte Quelle quantenentarteter Gase hohen Flusses für die Atominterferometrie unter Schwerelosigkeit’. Dissertation. Institut für Quantenoptik, Leibniz Universität Hannover, 2013 (cit. on p. 12).
86. A. Wenzlawski: ‘Matter-wave optics in microgravity: Laser technology and applications’. Dissertation. Departments Physik, Universität Hamburg, 2013 (cit. on p. 12).
87. M. Krutzik: ‘Matter wave interferometry in microgravity’. PhD thesis. Humboldt-Universität zu Berlin, Mathematisch-Naturwissenschaftliche Fakultät I, 2014 (cit. on p. 12).
88. J. Rudolph: ‘Matter-Wave Optics with Bose-Einstein Condensates in Microgravity’. Dissertation. Institut für Quantenoptik, Leibniz Universität Hannover, 2016 (cit. on p. 12).
89. A. Grote: ‘Ultracold 87Rb: from Quantum Metrology to Two-photon Ionisation’. Dissertation. Departments Physik, Universität Hamburg, 2016 (cit. on p. 12).
90. C. Grzeschik: ‘Experiments with Bose-Einstein Condensates in Microgravity’. Dissertation. Humboldt-Universität zu Berlin, 2017 (cit. on p. 12).
91. T. Sternke: ‘An ultracold high-flux source for matter-wave interferometry in microgravity’. Dissertation. Universität Oldenburg, 2018 (cit. on p. 12).
92. M. A. Popp: ‘Compact, low-noise current drivers for quantum sensors with atom chips’. Dissertation. QUEST-Leibniz-Forschungsschule, Leibniz Universität Hannover, 2018 (cit. on pp. 12, 22).
93. H. Ammann and N. Christensen: ‘Delta Kick Cooling: A New Method for Cooling Atoms’. *Physical Review Letters* (1997), vol. 78(2): pp. 2088–2091 (cit. on p. 12).
94. J. C. Camparo and R. P. Frueholz: ‘A dressed atom interpretation of adiabatic rapid passage’. *Journal of Physics B: Atomic and Molecular Physics* (1984), vol. 17(20): p. 4169 (cit. on p. 12).
95. S. M. Dickerson, J. M. Hogan, A. Sugarbaker, D. M. S. Johnson, and M. A. Kasevich: ‘Multiaxis Inertial Sensing with Long-Time Point Source Atom Interferometry’. *Phys. Rev. Lett.* (8 Aug. 2013), vol. 111: p. 083001 (cit. on p. 14).

96. P. Asenbaum, C. Overstreet, T. Kovachy, D. D. Brown, J. M. Hogan, et al.: ‘Phase shift in an atom interferometer due to spacetime curvature across its wave function’. *Physical review letters* (2017), vol. 118(18): p. 183602 (cit. on p. 14).
97. B. Barrett, L. Antoni-Micollier, L. Chichet, B. Battelier, T. Lévèque, et al.: ‘Dual matter-wave inertial sensors in weightlessness’. *Nature Communications* (2016), vol. 7: p. 13786 (cit. on p. 14).
98. G. Condon, M. Rabault, B. Barrett, L. Chichet, R. Arguel, et al.: ‘All-Optical Bose-Einstein Condensates in Microgravity’. *Phys. Rev. Lett.* (Dec. 2019), vol. 123: p. 240402 (cit. on pp. 14, 18).
99. A. Sugarbaker, S. M. Dickerson, J. M. Hogan, D. M. S. Johnson, and M. A. Kasevich: ‘Enhanced Atom Interferometer Readout through the Application of Phase Shear’. *Phys. Rev. Lett.* (11 Sept. 2013), vol. 111: p. 113002 (cit. on p. 14).
100. C. Overstreet, P. Asenbaum, T. Kovachy, R. Notermans, J. M. Hogan, et al.: ‘Effective Inertial Frame in an Atom Interferometric Test of the Equivalence Principle’. *Phys. Rev. Lett.* (18 May 2018), vol. 120: p. 183604 (cit. on p. 14).
101. S. Abend, M. Gebbe, M. Gersemann, H. Ahlers, H. Müntinga, et al.: ‘Atom-Chip Fountain Gravimeter’. *Phys. Rev. Lett.* (20 Nov. 2016), vol. 117: p. 203003 (cit. on p. 15).
102. M. Gebbe, J.-N. Siemß, M. Gersemann, H. Müntinga, S. Herrmann, et al.: ‘Twin-lattice atom interferometry’. *Nature communications* (2021), vol. 12(1): pp. 1–7 (cit. on p. 15).
103. M. Gersemann, M. Gebbe, S. Abend, C. Schubert, and E. M. Rasel: ‘Differential interferometry using a Bose-Einstein condensate’. *The European Physical Journal D* (2020), vol. 74(10): pp. 1–7 (cit. on p. 15).
104. J. Pahl, A. N. Dinkelaker, C. Grzeschik, J. Kluge, M. Schiemangk, et al.: ‘Compact and robust diode laser system technology for dual-species ultracold atom experiments with rubidium and potassium in microgravity’. *Applied Optics* (July 2019), vol. 58(20): p. 5456 (cit. on p. 15).
105. D. Guéry-Odelin, A. Ruschhaupt, A. Kiely, E. Torrontegui, S. Martinez-Garaot, et al.: ‘Shortcuts to adiabaticity: Concepts, methods, and applications’. *Reviews of Modern Physics* (2019), vol. 91(4): p. 045001 (cit. on pp. 17, 29).
106. S. van Frank, M. Bonneau, J. Schmiedmayer, S. Hild, C. Gross, et al.: ‘Optimal control of complex atomic quantum systems’. *Scientific reports* (2016), vol. 6(1): pp. 1–12 (cit. on pp. 17, 29).

107. S. Amri, R. Corgier, D. Sugny, E. M. Rasel, N. Gaaloul, et al.: ‘Optimal control of the transport of Bose-Einstein condensates with atom chips’. *Scientific reports* (2019), vol. 9(1): pp. 1–11 (cit. on pp. 17, 29).
108. C. Deppner, W. Herr, M. Cornelius, P. Stromberger, T. Sternke, et al.: ‘Collective-mode enhanced matter-wave optics’. *Phys. Rev. Lett.* (10 2021), vol. 127: p. 100401 (cit. on p. 17).
109. D. M. Farkas, E. A. Salim, and J. Ramirez-Serrano: ‘Production of rubidium bose-einstein condensates at a 1 hz rate’. *arXiv preprint arXiv:1403.4641* (2014), vol. (cit. on p. 18).
110. J.-F. Clément, J.-P. Brantut, M. Robert-De-Saint-Vincent, R. A. Nyman, A. Aspect, et al.: ‘All-optical runaway evaporation to Bose-Einstein condensation’. *Physical Review A* (2009), vol. 79(6): p. 061406 (cit. on p. 18).
111. T. Kinoshita, T. Wenger, and D. S. Weiss: ‘All-optical Bose-Einstein condensation using a compressible crossed dipole trap’. *Physical Review A* (2005), vol. 71(1): p. 011602 (cit. on p. 18).
112. K. Yamashita, K. Hanasaki, A. Ando, M. Takahama, and T. Kinoshita: ‘All-optical production of a large Bose-Einstein condensate in a double compressible crossed dipole trap’. *Physical Review A* (2017), vol. 95(1): p. 013609 (cit. on p. 18).
113. G. Colzi, E. Fava, M. Barbiero, C. Mordini, G. Lamporesi, et al.: ‘Production of large Bose-Einstein condensates in a magnetic-shield-compatible hybrid trap’. *Physical Review A* (2018), vol. 97(5): p. 053625 (cit. on p. 18).
114. R. Roy, A. Green, R. Bowler, and S. Gupta: ‘Rapid cooling to quantum degeneracy in dynamically shaped atom traps’. *Physical Review A* (2016), vol. 93(4): p. 043403 (cit. on p. 18).
115. S. Stellmer, B. Pasquiou, R. Grimm, and F. Schreck: ‘Laser cooling to quantum degeneracy’. *Physical review letters* (2013), vol. 110(26): p. 263003 (cit. on p. 18).
116. S. Bennetts, C.-C. Chen, B. Pasquiou, F. Schreck, et al.: ‘Steady-state magneto-optical trap with 100-fold improved phase-space density’. *Physical review letters* (2017), vol. 119(22): p. 223202 (cit. on p. 18).
117. C.-C. Chen, S. Bennetts, R. G. Escudero, B. Pasquiou, F. Schreck, et al.: ‘Continuous guided strontium beam with high phase-space density’. *Physical Review Applied* (2019), vol. 12(4): p. 044014 (cit. on p. 18).
118. S. Snigirev, A. J. Park, A. Heinz, I. Bloch, and S. Blatt: ‘Fast and dense magneto-optical traps for strontium’. *Physical Review A* (2019), vol. 99(6): p. 063421 (cit. on p. 18).

119. L. Hu, E. Wang, L. Salvi, J. N. Tinsley, G. M. Tino, et al.: ‘Sr atom interferometry with the optical clock transition as a gravimeter and a gravity gradiometer’. *Classical and Quantum Gravity* (2019), vol. 37(1): p. 014001 (cit. on p. 18).
120. J. Rudolph, T. Wilkason, M. Nantel, H. Swan, C. M. Holland, et al.: ‘Large momentum transfer clock atom interferometry on the 689 nm intercombination line of strontium’. *Physical review letters* (2020), vol. 124(8): p. 083604 (cit. on p. 18).
121. L. Badurina, E. Bentine, D. Blas, K. Bongs, D. Bortoletto, et al.: ‘AION: an atom interferometer observatory and network’. *Journal of Cosmology and Astroparticle Physics* (2020), vol. 2020(05): p. 011 (cit. on p. 18).
122. M. Abe, P. Adamson, M. Borcean, D. Bortoletto, K. Bridges, et al.: ‘Matter-wave Atomic Gradiometer Interferometric Sensor (MAGIS-100)’. *Quantum Science and Technology* (2021), vol. (cit. on p. 18).
123. A. Bertoldi, K. Bongs, P. Bouyer, O. Buchmueller, B. Canuel, et al.: ‘AEDGE: atomic experiment for dark matter and gravity exploration in space’. *Experimental Astronomy* (2021), vol.: pp. 1–10 (cit. on p. 18).
124. S. Loriani, D. Schlippert, C. Schubert, S. Abend, H. Ahlers, et al.: ‘Atomic source selection in space-borne gravitational wave detection’. *New Journal of Physics* (2019), vol. 21(6): p. 063030 (cit. on p. 18).
125. N. Heine, J. Matthias, M. Sahelgozin, W. Herr, S. Abend, et al.: ‘A transportable quantum gravimeter employing delta-kick collimated Bose–Einstein condensates’. *The European Physical Journal D* (2020), vol. 74(8): pp. 1–8 (cit. on p. 19).
126. K. Frye, S. Abend, W. Bartosch, A. Bawamia, D. Becker, et al.: ‘The Bose-Einstein condensate and cold atom laboratory’. *EPJ Quantum Technology* (2021), vol. 8(1): pp. 1–38 (cit. on pp. 19, 35).
127. S. T. Seidel: ‘Eine Quelle für die Interferometrie mit Bose-Einstein-Kondensaten auf Höhenforschungsraketen’. Dissertation. Institut für Quantenoptik, Leibniz Universität Hannover, 2014 (cit. on p. 22).
128. J. Grosse: ‘Thermal and Mechanical Design and Simulation for the first high precision Quantum Optics Experiment on a Sounding Rocket’. Dissertation. Universität Bremen, 2016 (cit. on p. 22).
129. V. Schkolnik: ‘Probing gravity with quantum sensors’. Dissertation. Humboldt-Universität zu Berlin, Mathematisch-Naturwissenschaftliche Fakultät, 2017 (cit. on p. 22).

130. A. Kubelka-Lange: ‘Entwicklung einer hocheffektiven Magnetfeldabschirmung für die Forschungsraketenmission MAIUS-1’. Dissertation. Universität Bremen, 2017 (cit. on p. 22).
131. M. D. Lachmann: ‘Materiewelleninterferenzen im Weltraum’. Dissertation. Institut für Quantenoptik, Leibniz Universität Hannover, 2020 (cit. on pp. 22, 31).
132. A. F. Palmerio, J. P. C. Peres da Silva, P. Turner, and W. Jung: ‘The development of the VSB-30 sounding rocket vehicle’. *European Rocket and Balloon Programmes and Related Research*. Vol. 530. 2003: pp. 137–140 (cit. on p. 22).
133. A. F. Palmerio, E. D. Roda, P. Turner, and W. Jung: ‘Results from the first flight of the VSB-30 sounding rocket’. *17th ESA Symposium on European Rocket and Balloon Programmes and Related Research*. Vol. 590. 2005: pp. 345–349 (cit. on p. 22).
134. H. Duncker, O. Hellmig, A. Wenzlawski, A. Grote, A. J. Rafipoor, et al.: ‘Ultrastable, Zerodur-based optical benches for quantum gas experiments’. *Applied optics* (2014), vol. 53(20): pp. 4468–4474 (cit. on p. 22).
135. B. Weps, D. Lüdtkke, T. Franz, O. Maibaum, T. Wendrich, et al.: ‘A Model-driven Software Architecture for Ultra-cold Gas Experiments in Space’. *69th International Astronautical Congress (IAC)*. Oct. 2018 (cit. on p. 22).
136. A. Kubelka-Lange, S. Herrmann, J. Grosse, C. Lämmerzahl, E. M. Rasel, et al.: ‘A three-layer magnetic shielding for the MAIUS-1 mission on a sounding rocket’. *Review of Scientific Instruments* (2016), vol. 87(6): p. 063101 (cit. on p. 23).
137. D. E. Pritchard: ‘Cooling neutral atoms in a magnetic trap for precision spectroscopy’. *Physical Review Letters* (1983), vol. 51(15): p. 1336 (cit. on p. 23).
138. German Aerospace Center (DLR): *Mobile rocket base - MORABA*. <https://moraba.de/en/> (cit. on p. 25).
139. L. Liu, D.-S. Lü, W.-B. Chen, T. Li, Q.-Z. Qu, et al.: ‘In-orbit operation of an atomic clock based on laser-cooled 87 Rb atoms’. *Nature communications* (2018), vol. 9(1): p. 2760 (cit. on p. 31).
140. E. Elliott, M. Krutzik, J. Williams, R. Thompson, and D. Aveline: ‘NASA’s Cold Atom Lab (CAL): system development and ground test status’. *NPJ Microgravity* (Dec. 2018), vol. 4(1): p. 16 (cit. on p. 31).
141. D. C. Aveline, J. R. Williams, E. R. Elliott, C. Dutenhoffer, J. R. Kellogg, et al.: ‘Observation of Bose–Einstein condensates in an Earth-orbiting research lab’. *Nature* (2020), vol. 582(7811): pp. 193–197 (cit. on p. 31).

142. N. Lundblad, R. A. Carollo, C. Lannert, M. J. Gold, X. Jiang, et al.: ‘Shell potentials for microgravity Bose-Einstein condensates’. *npj Microgravity* (Dec. 2019), vol. 5(1): p. 30 (cit. on p. 31).
143. M. Meister, A. Roura, E. M. Rasel, and W. P. Schleich: ‘The space atom laser: an isotropic source for ultra-cold atoms in microgravity’. *New Journal of Physics* (Jan. 2019), vol. 21(1): p. 013039 (cit. on p. 31).
144. R. A. Carollo, D. C. Aveline, B. Rhyno, S. Vishveshwara, C. Lannert, et al.: ‘Observation of ultracold atomic bubbles in orbital microgravity’. *arXiv preprint arXiv:2108.05880* (2021), vol. (cit. on p. 31).
145. Cold Atom Lab (CAL): *Quantum Technologies Take Flight*. <https://science.nasa.gov/technology/technology-highlights/quantum-technologies-take-flight> (cit. on p. 31).
146. B. Piest, M. D. Lachmann, W. Bartosch, D. Becker, J. Böhm, et al.: ‘MAIUS-2/-3: A system for two-species atom interferometry in space’. *24th ESA Symposium on European Rocket and Balloon Programmes and Related Research*. 2019 (cit. on p. 34).
147. B. Piest: ‘Bose-Einstein condensation of K-41 and Rb-87 on an atom chip for sounding rocket missions’. Dissertation. Institut für Quantenoptik, Leibniz Universität Hannover, 2021 (cit. on p. 34).
148. T. Lévèque, A. Gauguet, F. Michaud, F. Pereira Dos Santos, and A. Landragin: ‘Enhancing the Area of a Raman Atom Interferometer Using a Versatile Double-Diffraction Technique’. *Physical Review Letters* (Aug. 2009), vol. 103(8): p. 080405 (cit. on p. 34).
149. S.-w. Chiow and N. Yu: ‘Multiloop atom interferometer measurements of chameleon dark energy in microgravity’. *Physical Review D* (2018), vol. 97(4): p. 044043 (cit. on p. 35).

Curriculum Vitae

Personalien

Name Dennis Vincent Daniel Becker

Geburtstag, -ort 24.03.1988, Langenhagen

Schulbildung

2006 Allgemeine Hochschulreife
IGS Hannover-Linden

Studium

2006 - 2009 Physik - Bachelor of Science
Leibniz Universität Hannover

2009 - 2011 Physik - Master of Science
Leibniz Universität Hannover

2012 - 2021 Promotion am Institut für Quantenoptik
Leibniz Universität Hannover

Wissenschaftliche Publikationen

- M. D. Lachmann, H. Ahlers, **D. Becker**, A. N. Dinkelaker, J. Grosse, O. Hellmig, H. Müntinga, V. Schkolnik, S. T. Seidel, T. Wendrich, et al.: ‘Ultracold atom interferometry in space’. *Nature Communications* (2021), vol. 12: p. 1317.
- K. Frye, S. Abend, W. Bartosch, A. Bawamia, **D. Becker**, et al.: ‘The Bose-Einstein condensate and cold atom laboratory’. *EPJ Quantum Technology* (2021), vol. 8(1): pp. 1–38.
- A. Trimeche, B. Battelier, **D. Becker**, A. Bertoldi, P. Bouyer, et al.: ‘Concept study and preliminary design of a cold atom interferometer for space gravity gradiometry’. *Classical and Quantum Gravity* (2019), vol. 36(21): p. 215004.
- **D. Becker**, M. D. Lachmann, S. T. Seidel, H. Ahlers, A. N. Dinkelaker, J. Grosse, O. Hellmig, H. Müntinga, V. Schkolnik, T. Wendrich, et al.: ‘Spaceborne Bose-Einstein condensation for precision interferometry’. *Nature* (7727 2018), vol. 562: pp. 391–395.
- J. Grosse, S. T. Seidel, **D. Becker**, M. D. Lachmann, M. Scharringhausen, C. Braxmaier, and E. M. Rasel: ‘Design and qualification of an UHV system for operation on sounding rockets’. *Journal of Vacuum Science & Technology A: Vacuum, Surfaces, and Films* (2016), vol. 34(3): p. 031606.
- J. Rudolph, W. Herr, C. Grzeschik, T. Sternke, A. Grote, M. Popp, **D. Becker**, H. Müntinga, H. Ahlers, A. Peters, et al.: ‘A high-flux BEC source for mobile atom interferometers’. *New Journal of Physics* (2015), vol. 17(6): p. 065001.
- H. Müntinga, H. Ahlers, M. Krutzik, A. Wenzlawski, S. Arnold, **D. Becker**, K. Bongs, H. Dittus, H. Duncker, N. Gaaloul, et al.: ‘Interferometry with Bose-Einstein condensates in microgravity’. *Physical review letters* (2013), vol. 110(9): p. 093602.

Danksagung

An dieser Stelle möchte ich meinen Dank an all jene aussprechen, die zum Gelingen dieser Arbeit beigetragen haben und mich während dieser Zeit unterstützt haben. Dafür möchte ich mich als erstes bei Ernst und Wolfgang bedanken, die es mir ermöglicht haben, meine Doktorarbeit am Institut für Quantenoptik zu schreiben. Es war eine sehr besondere Zeit für mich und ich möchte mich dafür hier bei allen Mitgliedern des Institutes bedanken. Als nächstes möchte ich mich beim gesamten QUANTUS, MAIUS und BECCAL Team für die tolle Zusammenarbeit sowie beim DLR für die großartige Unterstützung bedanken. Ganz besonders möchte ich mich hier auch beim MAIUS-1 Team, den Kollegen der MORABA und der Esrange für die unvergessliche Raketenkampagne bedanken. Des Weiteren möchte ich denen danken, die mir bei der Korrektur der Arbeit oder formellen Fragen geholfen haben. Zu guter Letzt danke ich meinen Freunden und meiner Familie für die seelische Unterstützung während meiner Promotion.

Vielen Dank!

